



## *Kepler Data Release 6 Notes*

KSCI-19046-001

Data Analysis Working Group (DAWG)

*Jeffrey Van Cleve, Editor*

### Data Release 6 for Quarter Q4

Q.m		First Cadence MJD midTime	Last Cadence MJD midTime	First Cadence UT midTime	Last Cadence UT midTime	Num CINS
4	LC	55184.8778	55274.7038	12/19/09 21:04	3/19/10 16:53	4397
4.1	SC	55184.8679	55215.9262	12/19/09 20:49	1/19/10 22:13	45600
4.2	SC	55216.8056	55245.7389	1/20/10 19:20	2/18/10 17:44	42480
4.3	SC	55245.8009	55274.7137	2/18/10 19:13	3/19/10 17:07	42450

*Including uniformly reprocessed FFIs for Q0-Q4*

**FITS files may contain a few cadences outside the ranges shown above which should not be used for scientific analysis. See Section 2.1 for more details**

Prepared by: Jeffrey E Van Cleve Date 7/22/10  
Jeffrey Van Cleve, Kepler Science Office, for the DAWG (next page)

Approved by: Michael R. Haas Date 7/22/10  
*for* Jon Jenkins, Co-I for Data Analysis & DAWG Lead

Approved by: Michael R. Haas Date 7/22/10  
Michael R. Haas, Science Office Director

*(Faint mirrored text from the reverse side of the page is visible in the background)*

Star ID	Star Name	RA (J2000)	Dec (J2000)	Distance (pc)	Parallax (mas)	Proper Motion (mas/yr)	Radial Velocity (km/s)	Mass (solar)	Age (Myr)
1000000000000000000									
1000000000000000000									
1000000000000000000									
1000000000000000000									
1000000000000000000									
1000000000000000000									
1000000000000000000									
1000000000000000000									
1000000000000000000									
1000000000000000000									

These Notes are the collective effort of the Data Analysis Working Group (DAWG), composed of Science Office (SO), Science Operations Center (SOC), and Science Team (ST) members as listed below:

Jon Jenkins\*, Chair

Doug Caldwell\*, Co-Chair

Allen, Christopher L.

Bryson, Stephen T.

Clarke, Bruce D.

Cote, Miles T.

Dotson, Jessie L.

Gilliland\*, Ron (STSci)

Girouard, Forrest

Haas, Michael R.

Hall, Jennifer

Ibrahim, Khadeejah

Klaus, Todd

Kolodziejczak, Jeff (MSFC)

Li, Jie

McCauliff, Sean D.

Middour, Christopher K.

Quintana, Elisa V.

Tenenbaum, Peter G.

Twicken, Joe

Uddin, Akm Kamal

Van Cleve, Jeffrey

Wohler, Bill

Wu, Hayley Y.

\*Science Team

Affiliations are Kepler Science Office or Science Operations Center unless otherwise noted.

## Document Control

### Ownership

This document is part of the Kepler Project Documentation that is controlled by the Kepler Project Office, NASA/Ames Research Center, Moffett Field, California.

### Control Level

This document will be controlled under KPO @ Ames Configuration Management system. Changes to this document **shall** be controlled.

### Physical Location

The physical location of this document will be in the KPO @ Ames Data Center.

### Distribution Requests

To be placed on the distribution list for additional revisions of this document, please address your request to the Kepler Science Office:

Michael R. Haas  
Kepler Science Office Director  
MS 244-30  
NASA Ames Research Center  
Moffett Field, CA 94035-1000  
Michael.R.Haas@nasa.gov

## Table of Contents

<u><i>Prefatory Admonition to Users</i></u> .....	7
1. Introduction.....	8
2. Release Description .....	10
2.1 Summary of Contents .....	11
2.2 Pipeline Changes Since Previous Release.....	11
2.2.1 CAL: calibrated pixels .....	11
2.2.2 PA: uncorrected light curves and centroids .....	11
2.2.3 PDC: corrected light curves .....	12
3. Current Evaluation of Performance .....	13
3.1 Overall.....	13
3.2 Changes in Performance Since Previous Release .....	15
3.3 Known Calibration Issues .....	15
4. Data Delivered – Processing History.....	16
4.1 Overview .....	16
4.2 Pixel-Level Calibration (CAL).....	17
4.3 Photometric Analysis (PA) .....	18
4.4 Pre-Search Data Conditioning (PDC) .....	19
4.4.1 Description.....	20
4.4.2 Performance .....	21
4.4.3 Removal of Astrophysical Signatures .....	25
5. Lost or Degraded Data .....	28
5.1 Momentum Desaturation.....	28
5.2 Reaction Wheel Zero Crossings .....	29
5.3 Data Anomalies.....	31
5.3.1 Safe Mode .....	31
5.3.2 Loss of Fine Point.....	31
5.3.3 Pointing Drift and Attitude Tweaks.....	31
5.3.4 Downlink Earth Point .....	32
5.3.5 Manually Excluded Cadences .....	32
5.3.6 Anomaly Summary Table .....	32
5.4 Module 3 failure .....	33
5.5 Incomplete Apertures Give Flux and Feature Discontinuities at Quarter Boundaries.....	34
6. Systematic Errors .....	36
6.1 Argabrightening.....	36

6.2	Variable FGS Guide Stars .....	39
6.3	Pixel Sensitivity Dropouts .....	39
6.3.1	Particle-induced .....	40
6.3.2	Mod.out 4.2 performance discontinuity .....	41
6.4	Focus Drift and Jitter .....	42
6.5	Short Cadence Requantization Gaps .....	45
6.6	Spurious Frequencies in SC Data .....	46
6.6.1	Integer Multiples of Inverse LC Period .....	46
6.6.2	Other Frequencies .....	47
6.7	Known Erroneous FITS header keywords .....	49
7.	Data Delivered – Format .....	50
7.1	FFI .....	50
7.2	Light Curves .....	50
7.3	Pixels .....	51
7.4	Time and Time Stamps .....	52
7.4.1	Overview .....	52
7.4.2	Time Stamp Definitions .....	52
7.4.3	Caveats and Uncertainties .....	53
7.5	Future Formats Under Discussion .....	54
8.	References .....	55
9.	List of Acronyms and Abbreviations .....	56
10.	Contents of Supplement .....	59
10.1	Pipeline Instance Detail Reports .....	59
10.2	Thermal and Image Motion Data for Systematic Error Correction .....	59
10.2.1	Mod.out Central Motion .....	59
10.2.2	Average LDE board Temperature .....	60
10.2.3	Reaction Wheel Housing Temperature .....	60
10.2.4	Launch Vehicle Adapter Temperature .....	60
10.3	Background Time Series .....	60
10.4	Flight System Events .....	61
10.5	Calibration File READMEs .....	61

### ***Prefatory Admonition to Users***

The corrected light-curve product generated by Pre-search Data Conditioning (PDC) is designed to enable the Kepler planetary transit search. Although significant effort has been expended to preserve the natural variability of targets in the corrected light curves in order to enable astrophysical exploitation of the Kepler data, it is not possible to perfectly preserve general stellar variability on long timescales with amplitudes comparable to or smaller than the instrumental systematics, and PDC currently is known to remove or distort astrophysical features in a subset of the corrected light curves. In those cases where PDC fails, or where the requirements of an astrophysical investigation are in conflict with those for transit planet search, the investigator should use the uncorrected ('raw') light-curve product instead of the PDC ('corrected') light-curve product, and use the ancillary engineering data and image motion time series provided in the Supplement for systematic error correction. Investigators are strongly encouraged to study the Data Release Notes for any data sets they intend to use. The Science Office advises against publication of these Release 6 light curves without such careful consideration by the end user and dialog with the Science Office or Guest Observer Office as appropriate.

Users are encouraged to notice and document artifacts, either in the raw or processed data, and report them to the Science Office at [kepler-scienceoffice@lists.nasa.gov](mailto:kepler-scienceoffice@lists.nasa.gov).



*Users who neglect this Admonition risk seeing their works crumble into ruin before their time.*

## 1. Introduction

These notes have been prepared to give Kepler users of the Multimission Archive at STScI (MAST) a summary of flight system events which occurred during data collection that may impact quality, and a summary of the performance of the data processing pipeline used on that data set for this particular Release. The Notes for each release of data to the public archive will be placed on MAST along with other Kepler documentation, at [http://archive.stsci.edu/kepler/data\\_release.html](http://archive.stsci.edu/kepler/data_release.html).

The Notes are not meant to supplant the following documents, which are also needed for a complete understanding of the Kepler data:

1. **Kepler Instrument Handbook** (KIH, KSCI-19033) provides information about the design, performance, and operational constraints of the Kepler hardware, and an overview of the pixel data sets available. It was released on July 15, 2009, and is publicly available on MAST. Users will need to be familiar with the material in Sections 2 and 4.2-4.5 of the KIH to fully benefit from these Notes.
2. **Kepler Data Analysis Handbook** (KDAH) describes how these pixel data sets are transformed into photometric time series by the Kepler Science Pipeline, the theoretical basis of the algorithms used to reduce data, and a description of residual instrument artifacts after Pipeline processing. The initial release of the KDAH, focused on the needs of MAST users and Guest Observers (GOs), will be available in November, 2010. Until the KDAH is available, users seeking a discussion of Pipeline processing at a deeper level of detail than that provided in these Notes are directed to the SPIE papers (Refs. 3-5), which are available from MAST and will be available from SPIE (<http://spie.org/>) on or about 8/1/2010.
3. **Kepler Archive Manual** (KDMC-10008) describes file formats and the availability of data through MAST. The Archive Manual is available on MAST.
4. **Kepler Mission Special Issue of Astrophysical Journal Letters** (Volume 713, Number 2, 2010 April 20) contained several papers providing background on mission definition (Ref. 11), target selection (Ref. 12), science operations (Ref. 13), the Kepler point spread function (Ref. 14), instrument performance (Ref. 15), and the data processing pipeline (Ref. 9). Two papers discuss the characteristics of the Long Cadence data (Ref. 7), and Short Cadence data (Ref. 8) respectively. Numerous additional papers also provide early science results in both planet detections and asteroseismology, placing the use of Kepler data in context.

Users unfamiliar with the data processing pipeline should read Section 4 first, then the ApJ papers, then the SPIE papers. A list of acronyms and abbreviations appears in Section 9. Questions remaining after a close reading of these Notes and the Instrument Handbook may be addressed to [kepler-scienceoffice@lists.nasa.gov](mailto:kepler-scienceoffice@lists.nasa.gov).

A sentence at the start of a Section flags those Sections "recycled" from earlier Notes. If the Notes pertaining to a given data Release are revised, they will be reapproved for release and given an incremented document number KSCI-190XX-00n. n starts at 1 for the original version of the notes for a data Release. Reference to Release Notes will refer to the most recent version (highest n) unless otherwise stated.

Data which would be unwieldy to print in this document format are included in a tar file, the Data Release Notes Supplement, which has been released with this document. Supplement files are called out in the text, and a README file in the tar file also gives a brief description of the files contained. All supplement files are either ASCII or FITS format, though some are also provided as MATLAB \*.mat files for the convenience of MATLAB users. The contents of the Supplement are described in Section 10.



**Dates, Cadence numbers, and units:** Each set of coadded and stored pixels is called a *Cadence*, while the total amount of time over which the data in a Cadence is coadded is the *Cadence period*, which in the case of the flight default operating parameters is 1766 s = 0.49 h, or 270 frame times for Long Cadence, and 58.85 s or 9 frame times for Short Cadence. Cadences are absolutely and uniquely enumerated with *Cadence interval numbers* (CIN), which increment even when no Cadences are being collected, such as during downlinks and safe modes. The *relative Cadence index* (RCI) is the Cadence number counted from the beginning of a quarter (LC) or month (SC). RCIs are calculated from the first *valid* Cadence of a Quarter (LC) or Month (SC); as described in Section 2.1, FITS files may begin or end with a few invalid cadences. For example, the first LC of Q1 would have an RCI = 1 and CIN = 1105 while the last LC of Q1 has RCI = 1639 and CIN = 2743. Figures, tables, and supplement files will present results in CIN, RCI, or MJD, since MJD is the preferred time base of the Flight System and Pipeline, and can be mapped one-to-one onto CIN or RCI. On the other hand, the preferred time base for scientific results is Barycentric Julian Date (BJD); the correction to BJD is done on a target-by-target basis in the files users download from MAST, as described in detail in Section 7.4. Unless otherwise specified, the MJD of a Cadence refers to the time at the midpoint of the Cadence. Data shown will be for Q4, unless otherwise indicated in the caption. Flux time series units are always the number of detected electrons per Long or Short Cadence.

## 2. Release Description

A *data set* refers to the data type and observation interval during which the data were collected. The observation interval for Long Cadence data is usually a *quarter*, indicated by Q[n], though Q0 and Q1 are 10 days and one month, respectively, instead of 3 months as will be the case for the rest of the mission. Short Cadence targets can be changed every month, so SC observation intervals are indicated by Q[n]M[m], where m = 1 to 3 is the Month within that Quarter. The *data processing* descriptor is the internal Kepler Science Operations (KSOP) ticket used to request the data processing. The KSOP ticket contains a "Pipeline Instance Report," included in the Supplement, which describes the version of the software used to process the data, and a list of parameter values used. Released software has both a release label, typically of the form m.n, and a revision number (preceded by "r") precisely identifying which revision of the code corresponds to that label. For example, the code used to produce Data Release 6 has the release label "SOC Pipeline 6.1" and the revision number r37001. Unreleased software will, in general, have only a revision number for identification.

The same data set will, in general, be reprocessed as the software improves, and will hence be the subject of multiple releases. The combination of data set and data processing description defines a *data product*, and a set of data products simultaneously delivered to MAST for either public or proprietary (Science Team or GO) access is called a *data release*. The first release of data products for a given set of data is referred to as "new," while subsequent releases are referred to as "reprocessed."

Data products are made available to MAST users as FITS files, described in the Kepler Archive Manual and Section 7 of these Notes. While the Kepler Archive Manual refers to light curves which have not been corrected for systematic errors as 'raw', in these Notes they will be referred to as 'uncorrected' since the uncorrected light curves are formed from calibrated pixels, and 'raw' will refer only to the pixel values for which only decompression has been performed. The relationship of Pipeline outputs and MAST files is shown in Figure 2. The keyword `DATA_REL = 6` is in the FITS headers so users can unambiguously associate Release 6 FITS files with these Notes. In Release 6, all light curve files have FITS keyword `QUARTER = 4`.

Data Release 6 was produced with released code, with formal verification and validation of the pipeline and the resulting data products. While the Kepler data analysis Pipeline continues to evolve to adapt to the performance of the flight system and our understanding of the data, the rate of evolution is expected to be slower in the second year of the mission than in the first, with major upgrades on a roughly annual basis.

## 2.1 Summary of Contents

**Table 1: Contents of Release 6. CIN is the Cadence interval number described in Section 1. All Release 6 cadence data were processed under KSOP-479 with SOC Pipeline 6.1, revision number r37001, and are released for the first time. The Pipeline Instance ID (PID) for CAL, PA, and PDC is shown. Refer to Section 7.4 for a discussion of time and time stamps. All 4 channels of module 3 permanently failed at MJD 55205.72 (Section 5.4) and LC data are not available after that date. SC data for module 3 are available only for the first month.**

Q.m		CAL PID	PA PID	PDC PID	First Cadence MJD midTime	Last Cadence MJD midTime	CIN Start	CIN end	Num CINs
4	LC	1636	1676	1676	55184.8778	55274.7038	11914	16310	4397
4.1	SC	1756	1756	1756	55184.8679	55215.9262	345880	391479	45600
4.2	SC	2037	2037	2037	55216.8056	55245.7389	392770	435249	42480
4.3	SC	1876	1876	1876	55245.8009	55274.7137	435340	477789	42450

FITS files may contain a few cadences outside the ranges shown above; these Cadences do not have valid data, and contain either NaNs or real numbers inherited from earlier Pipeline runs. Such data are not part of Release 6 and should not be used for scientific analysis. For example, LC light curve FITS files contain 4420 Cadences, of which the first 23 are invalid. The CIN of the first valid Cadence is shown in Table 1, and the Relative Cadence Index in the Notes and Supplement is reckoned from that value.

For Release 6, all science mission FFIs have been uniformly reprocessed using Pipeline 6.1. With the exception of cosmic ray cleaning, which is not available for FFIs, the same CAL processing (Section 4) has been applied to these images as to the Release 6 cadence files. Science mission FFIs have time stamps commencing with 2009114174833 and use the same integration parameters as the Long Cadence science data. The “golden FFIs” between 2009114174833 and 2009116035924 were collected under conditions of excellent thermal and pointing stability, while the pointing for 2009170043915 is off by 4 pixels (16 arcsec) from the pointing established for the rest of Q2. FFIs are available from the MAST Kepler FFI search page: <http://archive.stsci.edu/kepler/ffi/search.php>.

## 2.2 Pipeline Changes Since Previous Release

This Section describes changes in the Pipeline code and parameters since the previous release (the Q0-Q1 data in Release 5). Changes are listed by Pipeline module outputs, and the corresponding data products on MAST. The software modules comprising the science data analysis Pipeline are described briefly in Section 4. Users unfamiliar with the Pipeline should read Section 4 before reading this Section. The PA and PDC versions and input parameters can be unambiguously referenced by their Pipeline Instance Identifier (PID), shown in Table 1.

### 2.2.1 CAL: calibrated pixels

No significant changes to CAL were made between Release 5 and Release 6.

### 2.2.2 PA: uncorrected light curves and centroids

There were no significant changes to PA between Release 5 and Release 6.

### 2.2.3 PDC: corrected light curves

There were no significant changes to PDC itself between Release 5 and Release 6. However, the following parameters were changed:

1. LDE board temperatures were used for cotrending, in addition to the motion polynomials, just as in Release 4 (Q3). In Release 5, only the motion polynomials were used.
2. The center-to-peak variability detection threshold was increased to 0.5% from 0.25%, restoring the value it had in Release 4 (Q3).
3. The buffer time around data anomalies for exclusion of giant planets was increased from 0.067 d to 0.1667 d. PDC will not allow giant transits to be identified for cadences within this buffer time before or after a safe mode, earth point, or attitude tweak, since the signatures so identified may not be real and marking them as such will prevent the systematic error correction from working properly in the vicinity of such known anomalies.

### 3. Current Evaluation of Performance

#### 3.1 Overall

The Combined Differential Photometric Precision (CDPP) of a photometric time series is the effective white noise standard deviation over a specified time interval, typically the duration of a transit or other phenomenon that is searched for in the time series. In the case of a transit, CDPP can be used to calculate the S/N of a transit of specified duration and depth. For example, a 6.5 hr CDPP of 20 ppm for a star with a planet exhibiting 84 ppm transits lasting 6.5 hours leads to a single transit S/N of  $4.1 \sigma$ .

The CDPP performance has been discussed by Borucki et al. (Ref. 2) and Jenkins et al. (Ref. 7). Jenkins et al. examine the 33.5-day long Quarter 1 (Q1) observations that ended 2009 June 15, and find that the lower envelope of the photometric precision on transit timescales is consistent with expected random noise sources. The Q4 data discussed in these Notes have the same properties, as shown in Figure 1. Nonetheless, the following cautions apply for interpreting data at this point in our understanding of the Instrument's performance:

1. Many stars remain unclassified until Kepler and other data can be used to ascertain whether they are giants or otherwise peculiar. Since giant stars are intrinsically variable at the level of Kepler's precision, they must be excluded from calculations of CDPP performance. A simple, but not foolproof, way to do this is to include only stars with high surface gravity ( $\log g > 4$ ).
2. Given the instrument artifacts discussed in detail in the KIH and Ref. 15, it is not generally possible to extrapolate noise as  $1/\sqrt{\text{time}}$  for those channels afflicted by artifacts which are presently not corrected or flagged by the Pipeline.
3. Stellar variability and many instrumental effects are not, in general, white noise processes.
4. There is evidence from the noise statistics of Q0 and Q1 (see the Release 5 Notes) that the Pipeline is overfitting the data for shorter data sets (a month or less of LC data) and fainter stars, so users are urged to compare uncorrected and corrected light curves for evidence of signal distortion or attenuation. The problem is less evident in the Q2-Q4 data sets than in the Q0 and Q1 data of Release 5.

Example published data is shown in [2] and [10].

The Transiting Planet Search (TPS) software module formally calculates CDPP on 6 hr timescales as a function of Cadence  $c$  for each target  $k$ . The temporal median of the CDPP for each target is  $\text{TMCDPP}_k = M_{\{c\}}(\text{CDPP}_{ck})$ , where  $M_{\{c\}}$  denotes the median over the set of Cadences  $\{c\}$ , which in this case is all the Cadences of a Quarter.  $\text{TMCDPP}_k$  is then divided by  $\sqrt{13/12}$  to approximate the results on the 6.5 hr benchmark time scale. The results (Figure 1) separate into two branches, mostly corresponding to giants with  $\log g < 4$  and dwarfs with  $\log g > 4$ .

$\text{TMCDPP}_k$  can be further summarized by aggregate statistics, which are calculated over all targets that are members of a set  $K$  satisfying certain criteria, such as the aggregate median  $\text{CDPP}_K = M_{\{k \in K\}}(\text{TMCDPP}_k)$ , where  $M_{\{k \in K\}}$  indicates the median calculated over all targets  $k$  satisfying the criteria for membership in  $K$ . For example,  $K$  can be {all targets with magnitude between 11.75 and 12.25 and  $\log g > 4$ }, loosely referred to as "12th magnitude dwarfs." Aggregate percentiles can be defined in the same way. Table 2 summarizes the results for Q4. Note that the median CDPP over  $K = \{\text{all stars in a given magnitude bin}\}$  actually decreases as stars get fainter beyond 10th magnitude since the proportion of all stars which are (quiet) dwarfs increases considerably as the stars get fainter.

The Jenkins et al. (Ref. 7) expression for the lower noise envelope was fitted to propagated uncertainties accounting for all known and quantified random errors such as shot noise from all

sources in the aperture (including background sky flux), read noise, quantization noise, and processing noise from pixel-level calibrations (such as the 1-D black and smear corrections). The errors appear to be dominated by shot noise out to Kepler magnitude =14 or so, and a simple way to think of the result is as the RSS sum of shot noise and an effective read noise corresponding to a source extracted from 2.6 pixels (given a per-frame, per pixel read noise of 100 e-). Extending this expression to the benchmark 6.5 hr transit time gives the results shown in Figure 1 and Table 2.

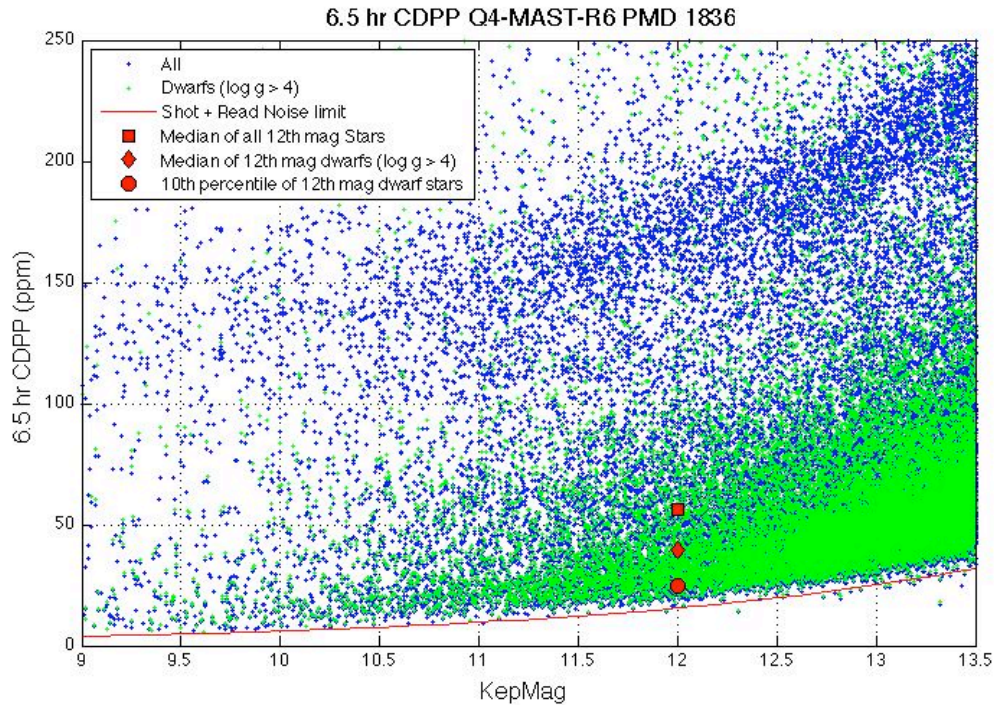


**Figure 1: 6.5 hr Temporal Median (TM) of the Quarter 4 CDPP time series calculated by the TPS Pipeline module for stars between 9th and 13.5th magnitude. The 6 hr TMCDDPs have been divided by  $\sqrt{13/12} = 1.041$  to approximate 6.5 hr TMCDDPs. Stars on the planetary target list with Kepler Magnitude < 13.5 and  $\log g > 4$ , which are almost certainly dwarf stars, are shown as green '+'s; other stars are marked with blue '+'s. The red line is the CDPP calculated from a simple shot and effective read noise model derived from Jenkins et al. (Ref. 7).**

**Table 2: Aggregate Statistics for the TMCDDPs plotted in Figure 1. Column Definitions: (1) Kepler Magnitude at center of bin. Bins are +/- 0.25 mag, for a bin of width 0.5 mag centered on this value. (2) Number of dwarfs ( $\log g > 4$ ) in bin. (3) 10th percentile TMCDDP for dwarfs in bin. (4) Median TMCDDP for dwarfs in bin. (5) Number of all stars in bin. (6) 10th percentile TMCDDP of all observed stars in bin. (7) Median TMCDDP for all stars in bin. (8) Simplified noise model CDPP, which does not include astrophysical noise. (9) Percentage of all observed stars with TMCDDP < noise model. TMCDDP is in units of ppm.**

center mag	number of dwarfs in bin	10th prc CDPP, dwarfs	median CDPP, dwarfs	number of all stars in bin	10th prc CDPP, all stars	median CDPP, all stars	simple Model CDPP	% of stars below model
9	29	9.2	42.2	174	11.3	84.8	3.8	0

center mag	number of dwarfs in bin	10th prc CDPP, dwarfs	median CDPP, dwarfs	number of all stars in bin	10th prc CDPP, all stars	median CDPP, all stars	simple Model CDPP	% of stars below model
10	161	11.9	36.6	539	13.8	93.2	6.0	0
11	630	18.5	35.3	1549	20.4	72.7	9.5	0.06
12	2222	24.6	39.5	3919	26.0	56.4	15.2	0.03
13	7009	36.3	51.2	10004	37.8	59.1	24.4	0.07

### 3.2 Changes in Performance Since Previous Release

Performance is essentially unchanged since Release 4 (Q3). In Release 6 (Q4), the median 12<sup>th</sup> magnitude dwarf had a CDPP of 40 ppm, while in Release 4 (Q3) this benchmark is 39 ppm.

### 3.3 Known Calibration Issues

Topics under consideration by the DAWG which may change future calibration parameters or methods include:

1. Find a set of ancillary engineering data (AED) and Pipeline-generated metrics which more effectively remove systematics errors without overfitting the data (and hence distorting the astrophysical signal). Correlations between the corrected light curves of different targets suggest the existence of unrepresented systematic errors.
2. Improve the characterization of stellar variability to represent weaker and more complex waveforms, so cotrending can be more effective when the stellar variability is temporarily removed from the light curve.
3. Characterize and correct for in-orbit change of focus (Section 6.3.2).
4. Identify particular light curves that are poorly corrected, and understand why generally effective remedies do not work in these cases. Feedback from users to [kepler-scienceoffice@lists.nasa.gov](mailto:kepler-scienceoffice@lists.nasa.gov) is essential for the SO and SOC to identify, flag, and fix all such "hard cases."
5. Mitigate or at least identify the Artifacts described in the KIH, Section 6.7.
6. Assess and improve the focal plane characterization models which are inputs to CAL.
7. Improve definition of photometric apertures, especially for saturated stars where failure to include pixels at the edge of charge bleeding columns can be particularly problematic (Section 5.5).

Calibration and data analysis issues related to the focal plane and its electronics are discussed in the Instrument Handbook.





algorithm. See Section 7 and the MAST Kepler Archive Manual for details of MAST file contents.

## 4.2 Pixel-Level Calibration (CAL)

*This section is unchanged since the Release 5 Notes, except as **highlighted**.*

The first step, pixel calibration (software module CAL), performs the pixel level calibrations shown in Figure 3. The SOC receives raw pixel data from each Kepler CCD, including collateral pixel data that is collected primarily for calibration. These collateral pixels include serial register elements used to estimate the black level (voltage bias), and masked and over-clocked rows used to measure the dark current and estimate the smear that results from the lack of a shutter on the spacecraft. Detailed models of each CCD have been developed from pre-flight hardware tests, along with full-frame images (FFIs) taken during commissioning prior to the dust cover ejection. These models are applied within CAL to correct for 2D bias structure, gain and nonlinearity of the ADU-to-photoelectron conversion, the electronic undershoot discussed in KIH Section 6.6, and flat field. CAL operates on long (30 min) and short (1 min) Cadence data, as well as FFIs [3, 9].

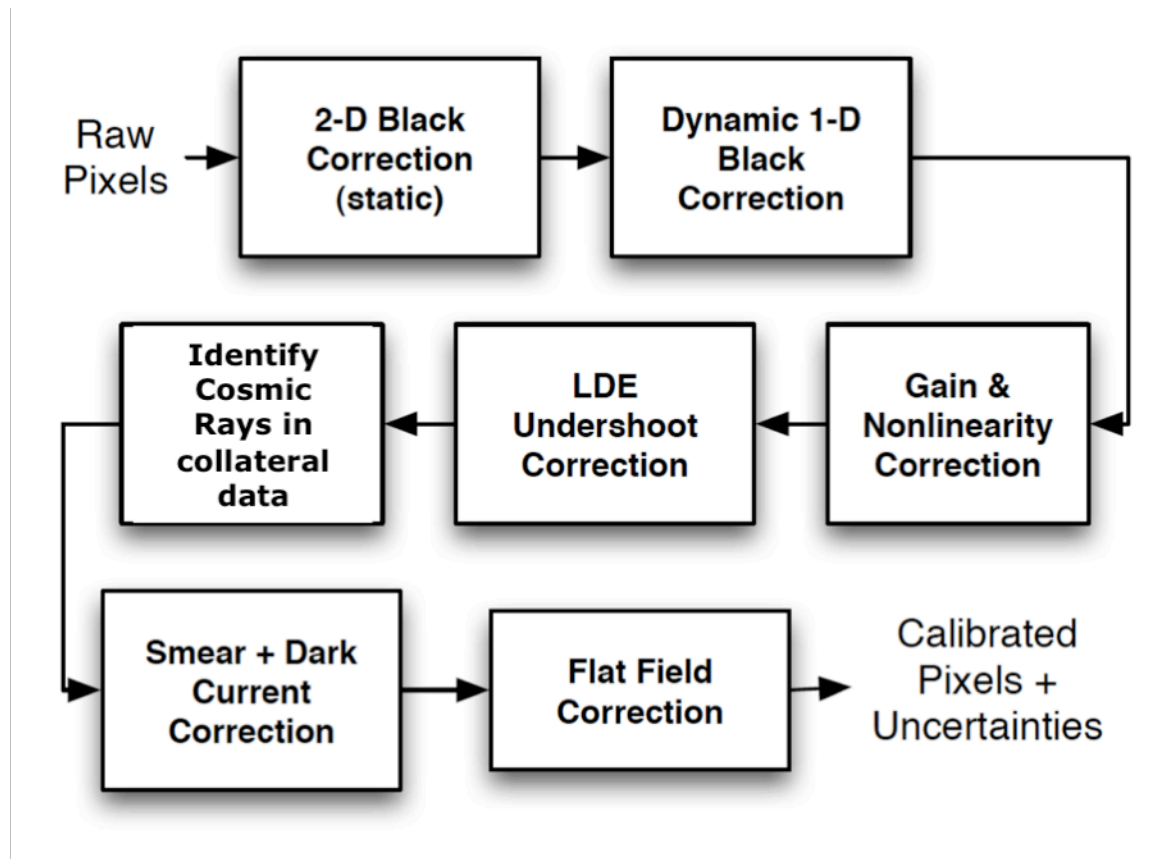


**Figure 3: Pixel Level Calibrations Performed in CAL.** See the Instrument Handbook for a discussion of signal features and image contents processed in CAL.

There may be rare cases where the bleeding smear value exceeds the 23 bits of the Science Data Accumulator. **Then the difference between the masked and virtual smear will toggle between positive and negative values, as a result of stellar variability or image motion, and CAL will produce incorrect results.** Users noticing repeated large step-like transitions between two

discrete flux levels should consult the FFIs to see whether either the masked or virtual smear regions contain bleeding charge. If so, please contact the Science Office for further investigation.

### 4.3 Photometric Analysis (PA)

*This Section is essentially unchanged from the Release 5 Notes, except to update Figure 4.*

The primary tasks of this module are to compute the photometric flux and photocenters (centroids) for up to 170,000 Long Cadence (thirty minute) and 512 Short Cadence (one minute) targets across the focal plane array from the calibrated pixels in each target's aperture, and to compute barycentric corrected timestamps per target and Cadence [4].

The tasks performed by Photometric Analysis (PA) are

1. Calculation of barycentric time correction, obviating the need for manual correction discussed in the Release 2 Notes (KSCI-19042).
2. Detection of Argabrightening events (Section 6.1). Argabrightening detection and associated Cadence gapping take place before CR detection; otherwise, many of the Argabrightening events would be cleaned as cosmic rays in the respective pixels, and not effectively detected and marked as data gaps.
3. Cosmic ray (CR) cleaning of background and target pixels, logging of detected CRs, and calculation of CR metrics such as hit rate and mean energy. The CR's are corrected by subtracting the residual differences after median filtering is performed on the detrended pixel time series. The same method and parameters are used for LC and SC. (Note 5)
4. Robust 2-D polynomial fitting to calibrated background pixels
5. Background removal from calibrated target pixels
6. Aperture photometry. In this Release, the flux is the sum of pixels in the optimal aperture after background removal (Simple Aperture Photometry, SAP).
7. Computation of flux-weighted (first moment) centroids. (Note 1).
8. Fitting of 2-D motion polynomials to target row and column centroids, which smoothly maps (RA,DEC) to (row, column) for a given output channel. (Note 4).
9. Setting gap indicators for Cadences with Argabrightening (Section 6.1). The gapped Cadences have all  $-\text{Inf}$  values in the FITS light curve files, except for the first three columns (see Section 7.2)

#### Notes

1. Flux-weighted (first moment) centroids are calculated for all targets. PRF centroids are also computed, but only for a small subset (PPA\_STELLAR) of the Long Cadence targets due to the heavy computational requirements of the PRF centroiding algorithm. The PRF fitting does not necessarily converge for targets which are faint, or located in complex fields. While only flux-weighted centroids are exported to MAST in this Release, they are suitable for precision astrometry [6] in uncrowded apertures. Users wishing to improve on the flux-weighted centroids need to consider the distribution of flux from non-target sources in the optimal aperture pixels or use the PRFs provided in the KIH Supplement to do their own fits.
2. There is no identification of bad pixels in PA in this Release, nor is there any exclusion, gapping or other treatment of known bad pixels. Bad pixels may be identified in future releases. The treatment of bad pixels is TBD, and may depend on how the pixel is bad (high read noise, unstable photoresponse, low photoresponse, etc.) and its location in the target aperture. While the Pipeline flags bad data on a per mod.out, per Cadence basis, bad pixels affect individual targets, and users are cautioned to carefully inspect the target pixels before believing peculiar light curves.
3. The output of PA is called 'raw' in the light curve FITS file, even though it is the sum of 'calibrated' pixels, because systematic errors have not been removed by PDC.
4. Motion polynomials are a means of estimating local image motion, and do not assume rigid body motion of the entire focal plane. They thus account for changes in plate scale, rotation,

image distortion, and differential velocity aberration (DVA) on a channel-by-channel and Cadence-by-Cadence basis (Figure 4). There is no requirement for smoothness in time of motion polynomials for cotrending and other purposes, and there is no fitting or smoothing across time (see Section 10.2.1 for further discussion). The simplified mod.out center motion time series provided in the Supplement are the row and column of the nominal center (in RA and DEC) of the mod.out as calculated from these motion polynomials.

5. Data which are greater than 12 median absolute deviations (MAD), after the removal of a trend formed by a quadratic fit followed by a 5 Cadence wide median filter, are identified as CRs. The MAD is calculated over a sliding window 145 Cadences wide after the trend is removed. The amplitude, Cadence, and location of the removed CR will be made available to users in future Releases, either as Cadence-to-Cadence cosmic ray correction tables, or integrated into the target pixel files (Section 7.5), so that users may restore the CRs and use their own methods of CR detection and removal if desired.

Astrophysical phenomena of only a single Cadence duration cannot be distinguished from CRs, as the Pipeline does not check for correlated outliers on adjacent pixels.

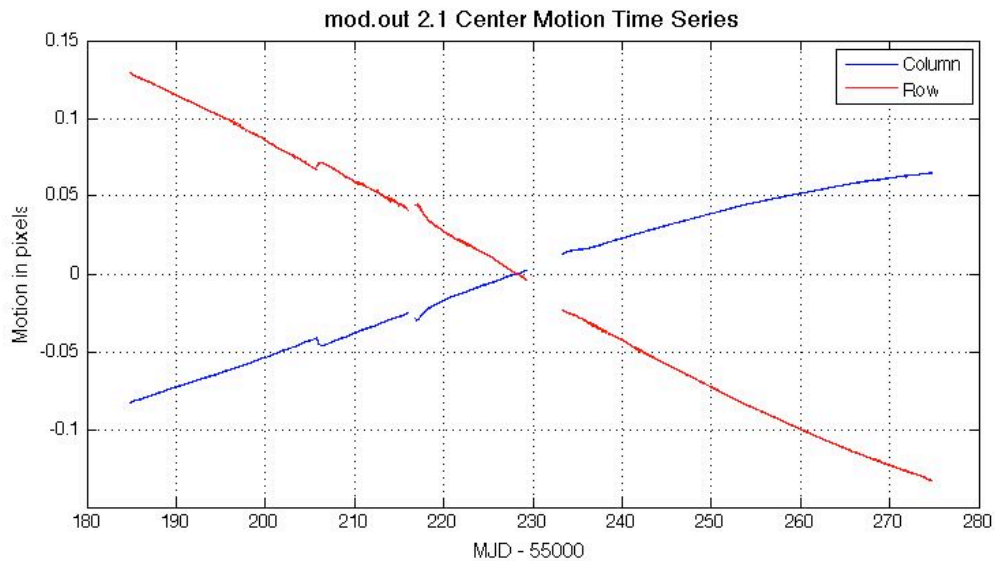


**Figure 4: Mod.out 2.1 Center Motion Time Series calculated from motion polynomials. The median row and column values have been subtracted. Since this mod.out is at the edge of the field, it shows large differential velocity aberration (DVA) with respect to the center of the field, as well as a higher sensitivity to focus jitter and drift. The motion on most channels shows a transient after module 3 failed at MJD = 55205.72, presumably due to the resultant change in CCD and electronics temperatures. The gap and subsequent motion transient at MJD = 55216.3 is a normal Earth point for downlink, while the gap between 55229.3 and 55233.3 was an unusually long Safe Mode. Except for these events, these curves are much smoother than those from Q1 (Release 5).**

#### 4.4 Pre-Search Data Conditioning (PDC)

*This Section is unchanged from the Release 5 Notes*

The primary tasks of PDC for MAST users are to correct systematic errors and remove excess flux in target apertures due to crowding. PDC also identifies outliers, and fills gaps in uncorrected flux light curves before passing the conditioned light curve to the Transiting Planet Search (TPS) component of the Pipeline for internal SOC use, but does not provide the outlier and gap fill results to MAST users. PDC was designed to remove systematic errors that are correlated with

ancillary engineering or Pipeline generated metrics (such as motion polynomials), and also to condition Long Cadence light curves for the transiting planet search (TPS). Significant effort has been expended to preserve the natural variability of targets, though further effort is still required to strike the right balance between preserving stellar variability signals and removing signatures correlated with instrumental effects. Users will therefore need to be cautious when their phenomena of interest are much shorter ( $<1$  h) or much longer ( $>5$  d) than a transit, or have complex light curves with multiple extrema on transit time scales (such as eclipsing and contact binaries). Examples of astrophysical features removed or significantly distorted by PDC are shown in Section 4.4.3.

Tuning the parameters of PDC requires assessing the relative merits of removing instrumental artifacts, preserving transits and their shapes, and preserving other astrophysical phenomena, and it is not likely that any single choice can give satisfactory results for all observing conditions, targets, and phenomena of interest. Hence, PDC is discussed in greater detail in these Notes than is CAL or PA. Users concerned about the impact of PDC on their signals of interest are invited to use the ancillary engineering data (AED) and motion time series in the Supplement to perform their own systematic error correction.

#### 4.4.1 Description

*This Section is unchanged from the Release 5 Notes.*

The tasks performed by PDC are:

1. Accept data anomaly flags for Cadences which are known to be lost or degraded (Section 4.4.2). These Cadences and their corresponding data anomalies are shown in Section 5.3.6
2. Resampling of AED to match the sampling rate of LC and SC data.
3. Identification and correction of unexplained discontinuities (i.e. unrelated to known anomalies), an iterative process.
4. Cotrend target flux time series against AED and motion polynomials derived by PA (Section 4.3 item 8) to remove correlated linear and nonlinear deterministic trends. Singular Value Decomposition (SVD) is used to orthogonalize the set of basis vectors and numerically stabilize the model fit.
5. Identify variable stars ( $>0.5\%$  center-peak variability).
6. For variable stars only, perform coarse systematic error correction with the following steps:
  - a. Correct discontinuities due to attitude tweaks.
  - b. Compare phase-shifting harmonic fitting to simple polynomial fitting, and select the method which gives the smallest error for initial detrending.
  - c. Correct thermal recovery transients with a polynomial fit for each target.
  - d. Remove a low-order polynomial trend from the transient-corrected light curve
  - e. Repeat the harmonic fit first done in Step 6.b, and save this improved harmonic fit for later restoration.
  - f. Subtract the improved harmonic fit from the light curve resulting from Step 3, and cotrend the harmonic-removed light curve as in Step 4.
7. For stars initially identified as variable, if the standard cotrended result is not variable and cotrending has reduced the noise then the identification of the star as variable is considered mistaken. Then the result of the standard cotrending is retained. Otherwise, the result of the harmonic free cotrending is retained. The harmonic content is restored later in PDC.
8. Assess results of cotrending. If cotrending has increased the noise by  $>5\%$ , restore the uncorrected light curve at this point.
9. Correction for the excess flux in the optimal aperture for each target due to crowding, as calculated over the optimal aperture.
10. Identification and removal of impulsive outliers after masking off astrophysical events such as giant transits, flares, and microlensing. A median filter is applied to the time

series after the removal of obvious astrophysics, and the residual is determined by subtracting the median series from the target flux series. A robust running mean and standard deviation of the residual is calculated and points more than  $12 \sigma$  (LC) or  $8 \sigma$  (SC) from the mean are excluded. Not all astrophysical events are successfully masked, and hence may be falsely identified as outliers or may unnecessarily increase the noise threshold for outliers. The masked events are restored to the MAST corrected light curves.

#### Notes

1. The crowding metric is the fraction of starlight in an aperture which comes from the target star. For example, a crowding metric of 1 means that all the light in an aperture comes from the target, so the light curve needs no correction. A crowding metric of 0.5 means that half the light is from the target and half from other sources, so the flux must be decreased by half before the correct light curve for the target is obtained. Note that the uncorrected flux time series are *not* corrected for crowding. The crowding metric is based on the Kepler Input Catalog (KIC) star locations and brightnesses, the local PRF of the target star and its neighbors, and the optimal aperture. It is averaged over a Quarter, and neglects seasonal and secular changes in the PRF compared to the model established by observations during Commissioning. A given star will move to different parts of the Kepler focal plane from Quarter to Quarter as Kepler rolls, so the PRF, aperture, and crowding metric will also vary from Quarter to Quarter.
2. Gaps are not filled in the MAST files, and are represented as -Infs. Intermediate data products generated by PDC and internal to the SOC do have gaps filled, before being passed to planetary search parts of the Pipeline.
3. Different frequencies of AED will physically couple to the photometric light curve with different strengths. PDC represents this by decomposing AED time series into low and high bandpass components, and allowing the coefficients of the components to vary independently in the fit.
4. The output of PDC is referred to as 'corrected' data in the delivered files. Users are cautioned that systematic errors remain, and their removal is the subject of ongoing effort as described in Section 3.3.

#### **4.4.2 Performance**

*This Section is conceptually unchanged from the Release 4 and 5 Notes. It has been modified to show examples from Q4. Cases where the examples are not from Q4 are labeled as such in the captions.*

PDC gives satisfactory results on most stars which are either intrinsically quiet (Figure 5), or have well-defined harmonic light curves above the detection threshold (Figure 6); in most of these cases, the standard deviation of the corrected flux is within a factor of 2 of the noise expected from read and shot noise in the calibrated pixels summed to form the uncorrected light curve. It also performs well in many cases where the star is variable, but without a dominant harmonic term (Figure 7). However, PDC will sometimes not identify a target-specific discontinuity (Figure 8), and will sometimes introduce noise into complex lightcurves (Figure 9). Conversely, PDC sometimes identifies eclipses as discontinuities and introduces a discontinuity in an attempt to correct the false discontinuity (Figure 10).

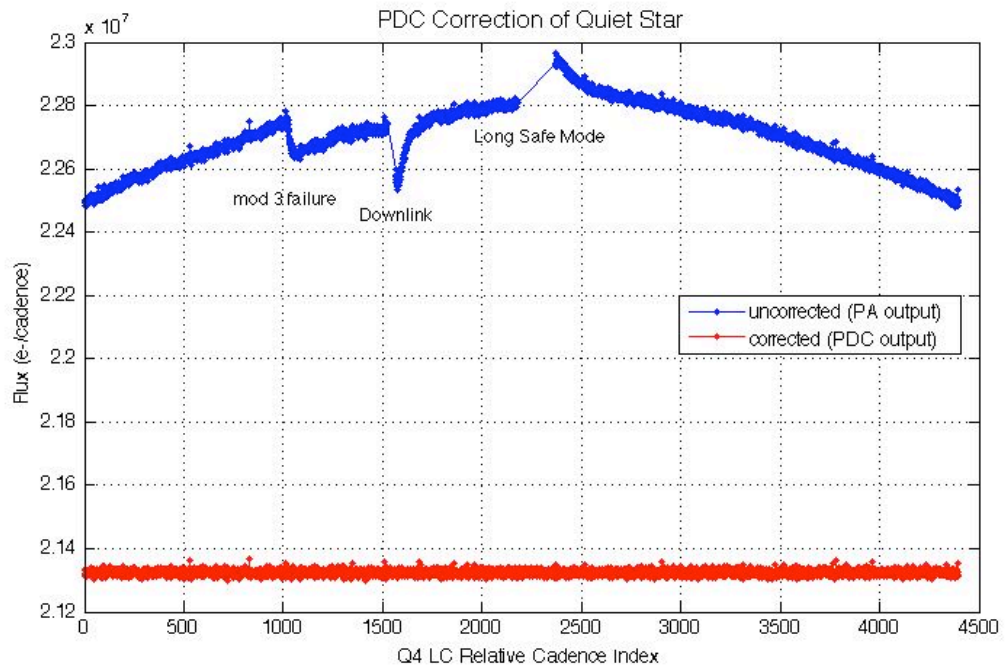


**Figure 5: Q4 example of PDC removal of trends and discontinuities from the light curve of a quiet star of Kepler magnitude 14.6. The noise in the corrected light curve is only 13% greater than the noise expected from the calibrated pixels, a considerable improvement over the uncorrected light curve.**

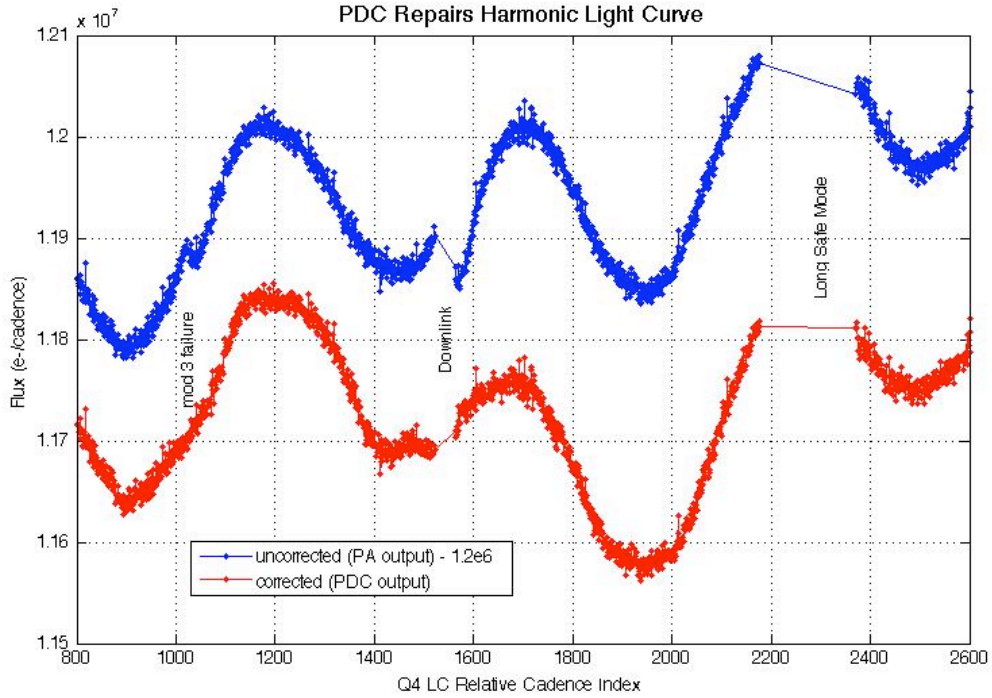


**Figure 6: Q4 example of PDC correction of a harmonically variable star. MAST users receive the light curve corrected for systematic errors, with the harmonic variability restored and gaps in the data represented by -Infs. The corrected light curve delivered to MAST is shown in red in this Figure.**

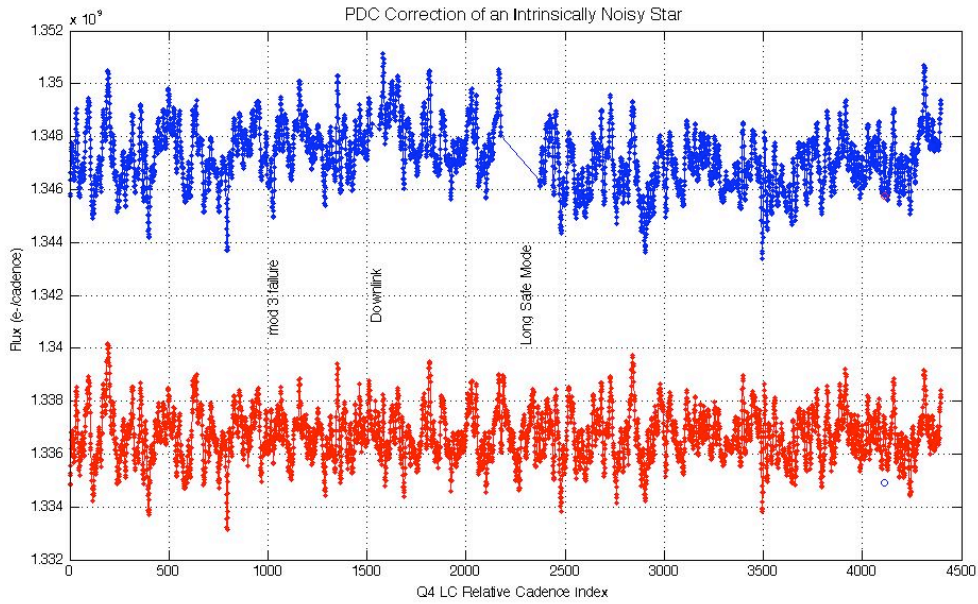


**Figure 7: Q4 example of PDC correction of a non-harmonically variable star. The RMS of the corrected (red) curve is about 25x the noise calculated from the read and shot noise in**

the calibrated pixels, and is believed to be almost entirely due to intrinsic stellar variability. While this figure illustrates PDC's ability to fill data gaps, such as during the long safe mode, the filled data is not delivered to MAST and users will have  $-\text{Inf}$  for the flux of those cadences.

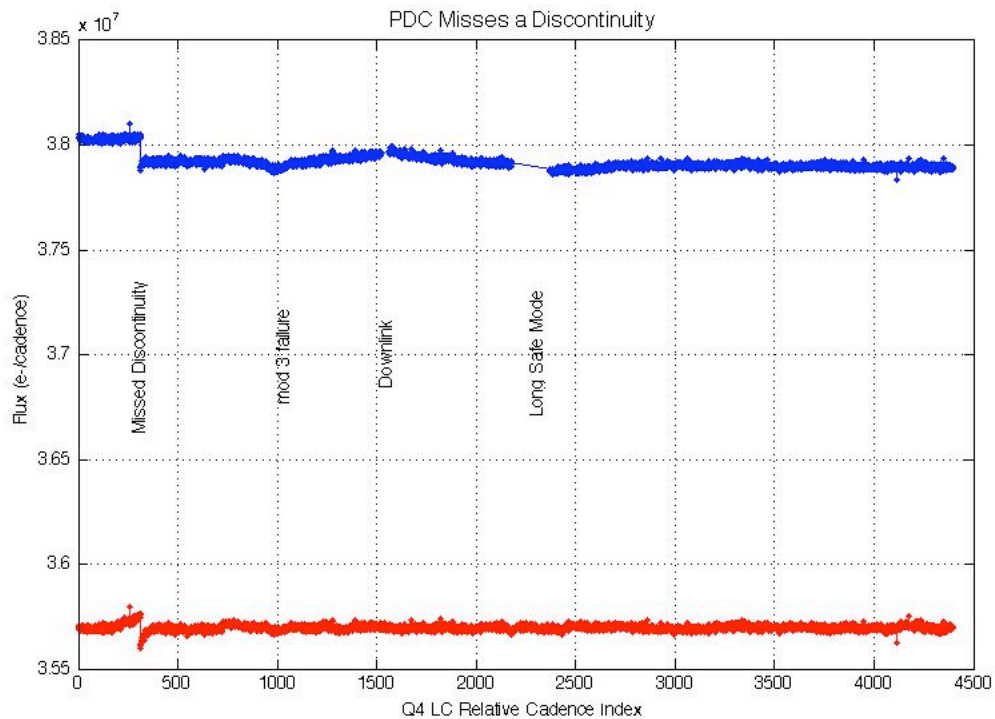


**Figure 8: Q4 example of an unidentified and hence uncorrected target-specific discontinuity.**



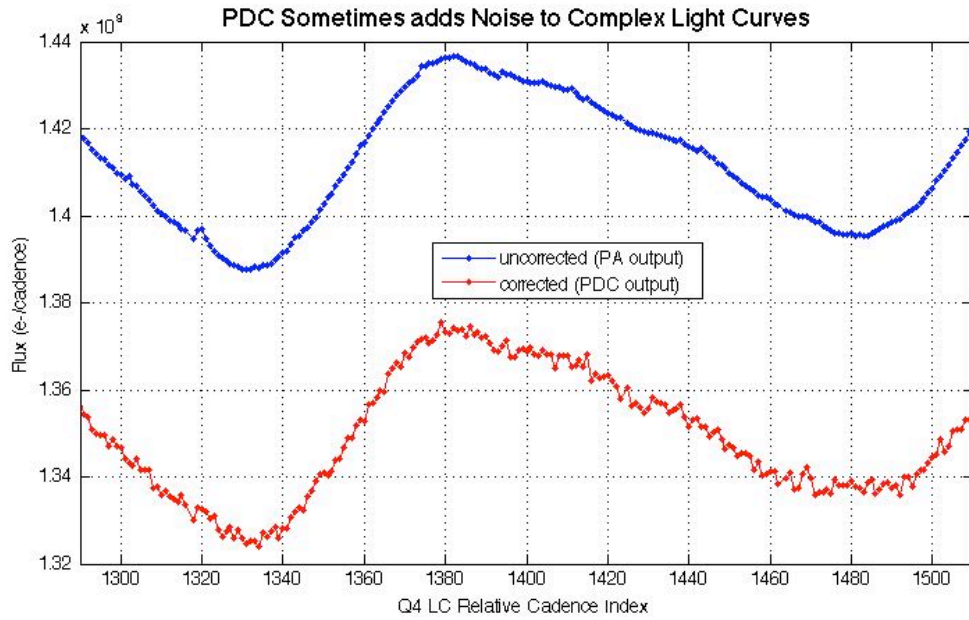


**Figure 9: Q4 example of PDC adding short-period noise to a light curve, which it did not identify as a bad cotrend.**

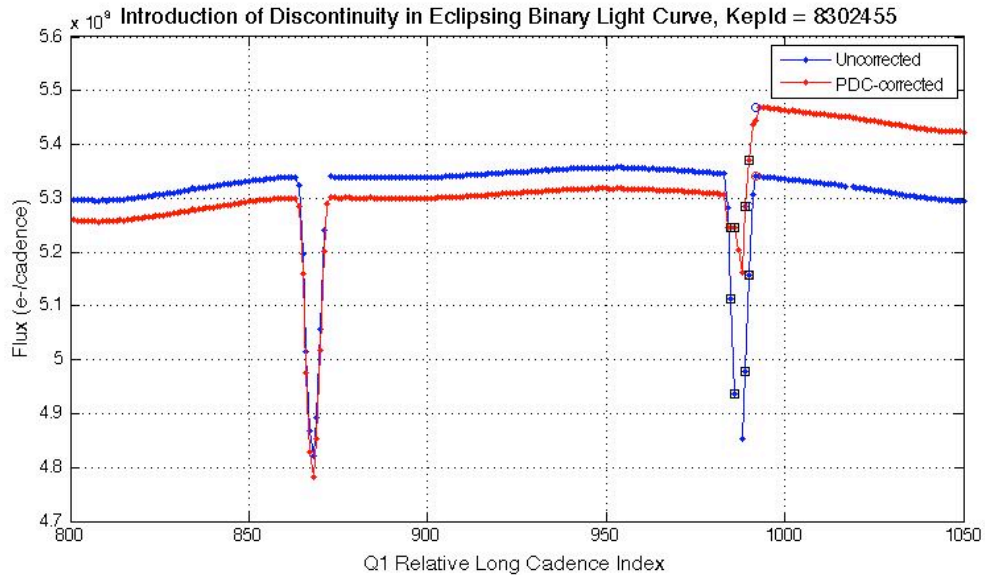


**Figure 10: Q1 Release 5 example of PDC misidentifying an eclipse as a discontinuity, and mistakenly introducing a discontinuity into the 'corrected' light curve.**

#### 4.4.3 Removal of Astrophysical Signatures

*This Section is conceptually unchanged from the Release 5 Notes. It has been modified to show examples from Q4. Cases where the examples are not from Q4 are labeled as such in the captions.*

PDC can remove astrophysical signatures if they are:

1. Harmonic, but have periods  $> 5d$  and fall below PDC's detection threshold for stellar variability. In Release 6, the center-peak threshold is 0.5%, which for otherwise quiet stars allows a harmonic with a peak-to-peak amplitude of 1.0% to go undetected.
2. Spikes a few Cadences wide (Figure 12), such as flares, or other steep gradients in flux.
3. More or less linear ramps over the processing interval.
4. Harmonic signals above the threshold, but the harmonic fit does not produce a good fit, and current algorithm fails to recognize that cotrending has performed badly.
5. Non-harmonic signals for which current algorithm fails to recognize that cotrending has performed badly.
6. Harmonic signals above the threshold for which the fit is good, but PDC incorrectly determines that target was cotrended well when treated as non-variable (Figure 11).

A thorough study of astrophysical signal distortion by PDC is planned, but has not been performed to date. Users may be helpful to this effort by reporting light curves, in which they suspect that a signal has been distorted or removed, to the Science Office at [kepler-scienceoffice@lists.nasa.gov](mailto:kepler-scienceoffice@lists.nasa.gov).

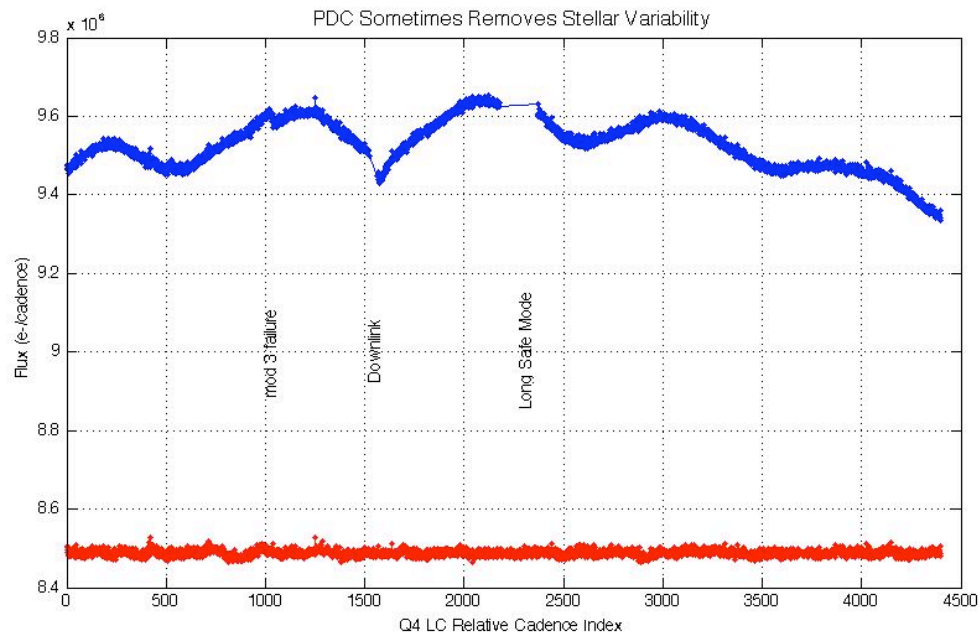


**Figure 11: Q4 example of PDC removal of harmonic stellar variability. The amplitude of the variability is  $\pm 0.6\%$ , slightly exceeding the threshold of  $\pm 0.5\%$ , before initial cotrending. Standard cotrending eliminated the variability but increased the noise, which PDC did not detect in this case. As described in Section 4.4.1 Step 7, if PDC had detected the increase in noise, it would have retained the result of the harmonic-removed cotrending, and restored the harmonic content before export to MAST.**

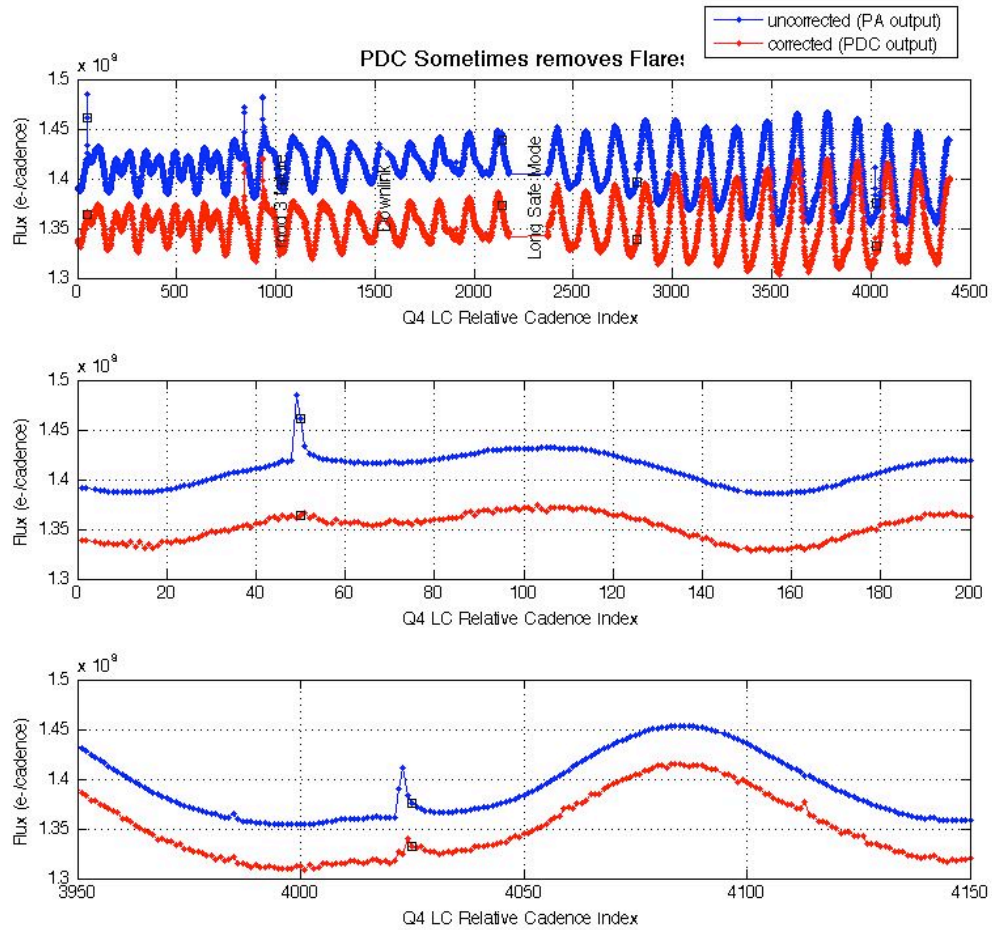


**Figure 12: Q4 example of astrophysical events, possibly flares, identified by PDC and removed from the corrected light curve. The upper panel shows the whole Quarter, while the lower two panels zoom in on the events removed. Open black squares show astrophysical events identified as discontinuity anomalies and “corrected.” Unlike outliers, discontinuities are *not* restored to the light curves before delivery to MAST. Note that few-cadence events near RCI = 838 and 935 are not identified as discontinuities.**

## 5. Lost or Degraded Data

In this Section, we discuss Cadences which are essentially lost to high-precision photometry due to planned or unplanned spacecraft events. Particularly important and unexpected phenomena are written up as Kepler Anomaly Reports (KARs), or mitigated by SOC change requests (KSOCs). Puzzling features of the data products, which do not succumb to cursory examination by the DAWG, are written up as K-DAWG tickets to initiate and track more thorough investigations.

Significant data loss events which occurred for the first time in Q4 include the permanent loss of module 3 (Section 5.4) and a Safe Mode of almost 4 days duration (Section 5.3.1)

### 5.1 Momentum Desaturation

Solar radiation torque causes angular momentum to build up in the reaction wheels, which then must be desaturated by thruster firings when the wheels spin up to their maximum operating RPM. Desats occur every 3 days. The spacecraft (S/C) is not designed to maintain Fine Point control during these events, and enters Coarse Point mode. The subsequent image motion is sufficient to spoil the photometric precision of data collected during desats, and a few minutes after desats during which the spacecraft restores Fine Point control. One LC and several SCs are affected for each desaturation.

The momentum dump Cadences have -Infs in the delivered light curve files, but finite values in the uncalibrated and calibrated pixels. The dump Cadences are listed in Table 3 so that users of time series will know which -Infs are due to desats, and users of pixel data will know which Cadences to exclude from their own analyses. Tables of the more numerous SCs afflicted by desats is included in the Supplement, though they duplicate some of the information in the SC data anomaly tables (Section 5.3.6).

**Table 3: Momentum dumps in Q4 and the corresponding Long Cadences. CIN = Cadence Interval Number, RCI = Relative Cadence Index.**

Q4 LC	CIN	RCI	Date(MJD)
	11916	3	55184.91860
	12062	149	55187.90191
	12208	295	55190.88521
	12354	441	55193.86852
	12500	587	55196.85182
	12646	733	55199.83513
	12792	879	55202.81843
	12938	1025	55205.80174
	13084	1171	55208.78505
	13230	1317	55211.76835
	13376	1463	55214.75166
	13429	1516	55215.83464
	13575	1662	55218.81794
	13721	1808	55221.80125
	13867	1954	55224.78455
	14013	2100	55227.76786
	14352	2439	55234.69485
	14498	2585	55237.67816
	14644	2731	55240.66146
	14790	2877	55243.64477
	14839	2926	55244.64601
	14985	3072	55247.62932

15131	3218	55250.61262
15277	3364	55253.59593
15423	3510	55256.57924
15569	3656	55259.56254
15715	3802	55262.54585
15861	3948	55265.52915
16007	4094	55268.51246
16153	4240	55271.49576
16299	4386	55274.47907

## 5.2 Reaction Wheel Zero Crossings

*The descriptive part of this Section is conceptually unchanged since Release 4 (Q3). The Figure has been updated to show a Q4 example, and the Table shows the zero crossing times for Q4.*

Another aspect of spacecraft momentum management is that some of the reaction wheels cross zero angular velocity from time to time. The affected wheel may rumble and degrade the pointing on timescales of a few minutes. The primary consequence is an increased noise in the Short Cadence centroids, and pixel and flux time series. The severity of the impact to the SC flux time series seems to vary from target to target, with all SC targets showing some impact on the centroid and pixel time series. In some cases, we observe negative spikes of order  $10^{-3}$  to  $10^{-2}$  in SC relative flux time series (Figure 13), and these Cadences must be excluded from further analysis. The impact on Long Cadence data is much less severe in both amplitude and prevalence. Zero crossings are not gapped in this Release, and users will have to use Table 4 to identify possibly afflicted Cadences.

In Figure 13, the noise in centroids, and loss of flux, occurs on multiple stars during the zero crossing, so this noise is not the result of an uncorrected cosmic ray event or other local transient. Neither is it due to the momentum dumps (Section 5.1) labeled in the Figure, for which one or two Cadences right after the dump may have bad pointing, but are not flagged as data gaps by the Pipeline. The zero crossings occur at distinctly different times than the momentum dumps.

Since the Pipeline does not flag zero crossings as anomalous data, the zero crossing events are shown in Table 4. Events were identified in reaction wheel telemetry, which is not sampled synchronously with Cadences. For each zero crossing event, the last Cadence ending before the event and the first Cadence beginning after the event were identified. Overlap between events is due to this rounding of Cadence numbers at times when the slowest wheel had nonzero speed for a time interval shorter than 2 Cadence periods.

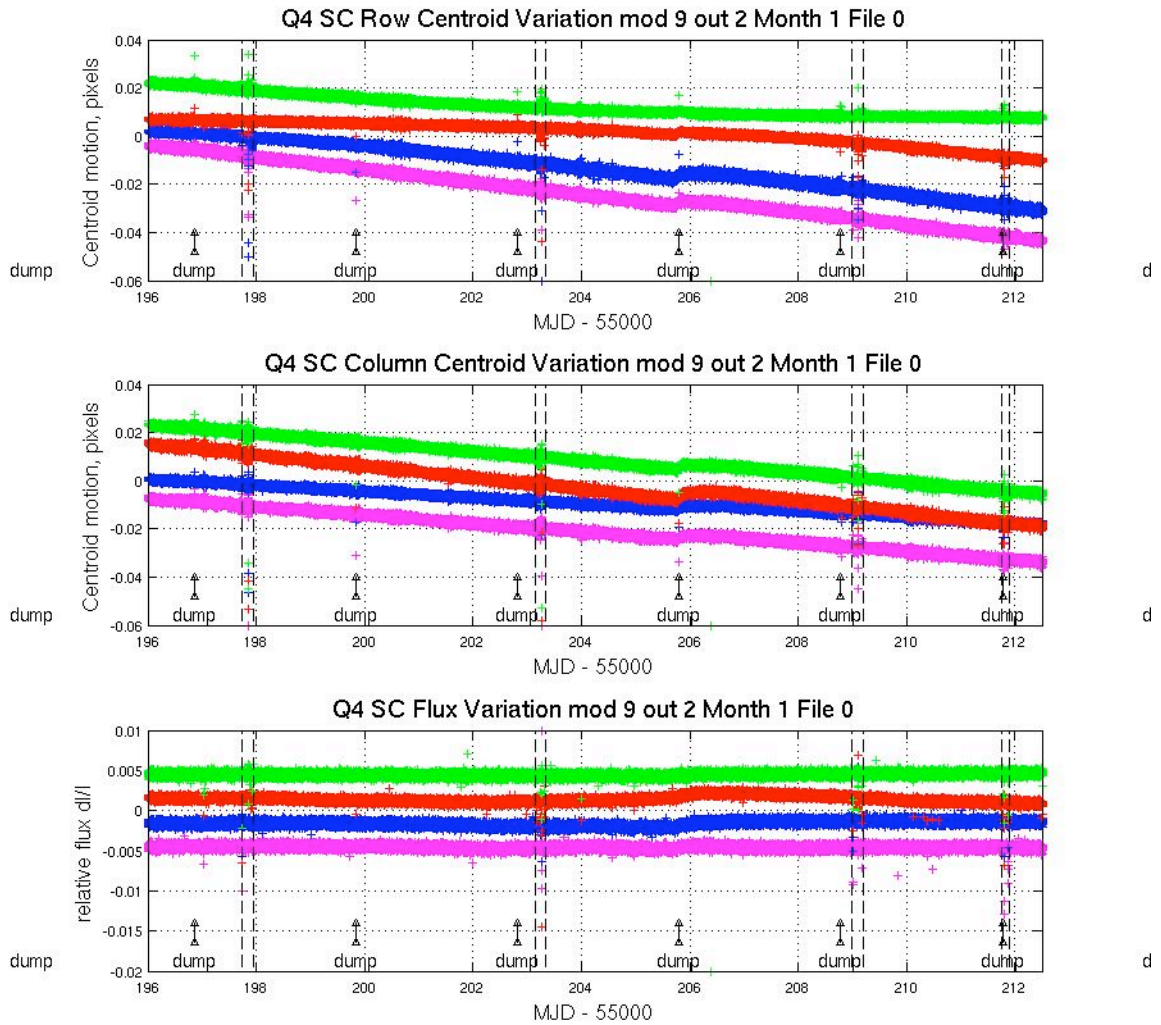


**Figure 13: Example from Q4 of the effect of reaction wheel speed zero crossing on SC flux and centroids. The plots show row and column centroid motion, and the relative flux change, in the neighborhood of zero crossings. The data on several stars are overlotted in different colors in each panel of the Figure. Vertical dashed black lines bracket the times during which at least one wheel had zero speed according to its telemetry. The curves are offset for clarity, and momentum dumps are labeled. The kink in the data at MJD = 55205.72 is the failure of mod 3.**

**Table 4: Zero crossing events in Q4, defined as the time from first to last zero crossing in the event, rounded to the nearest Cadence.**

Column Definitions			Cadence Interval Numbers			
LC	midTime	MJD	Long Cadence		Short Cadence	
Event#	Start	End	Start	End	Start	End
1	55197.730	55197.955	12543	12554	364765	365081
2	55203.145	55203.350	12808	12818	372736	372994
3	55208.989	55209.194	13094	13104	381296	381589
4	55211.748	55211.891	13229	13236	385368	385541
5	55214.874	55215.017	13382	13389	389944	390129
6	55268.778	55269.003	16020	16031	469080	469397
7	55271.782	55271.925	16167	16174	473503	473691

### 5.3 Data Anomalies

#### 5.3.1 Safe Mode

From time to time, the Kepler Spacecraft will go into Safe Mode, because of an unanticipated sensitivity to cosmic radiation, or unanticipated responses to command sequences. While each individual event is unexpected, it is not unusual for newly-commissioned spacecraft to experience them, until the in-orbit idiosyncrasies of the flight system are understood. Kepler's Flight Software has been modified to leave the LDE on during radiation-induced resets of the RAD750 processor, so that data degradation due to thermal transients after an LDE power cycle does not occur during this kind of Safe Modes.

The longest Safe Mode to date occurred in Q4, between MJD = 55229.3515 and 55233.3156, almost 4 days. This was not a radiation-induced reset, so the LDE was off during the Safe Mode.

#### 5.3.2 Loss of Fine Point

From time to time, the Kepler spacecraft will lose fine pointing control, rendering the Cadences collected useless for photometry of better than 1% precision. While the LOFPs are treated as lost data by the Pipeline, users with sources for which ~1% photometry is scientifically interesting may wish to look at the pixel data corresponding to those Cadences. Recent Flight Software upgrades have greatly reduced the frequency and duration of LOFPs.

There were no LOFPs in Q4.

#### 5.3.3 Pointing Drift and Attitude Tweaks

Daily reference pixels are used by the SOC/SO to measure S/C attitude. The SOC PDQ software uses centroids of 3-5 stars per module/output to determine the measured boresight attitude compared with the pointing model (which accounts for differential velocity aberration). The Photometer Attitude Determination (PAD) software performs a similar calculation to reconstruct the attitude using the Long Cadence science data when the data are processed after each downlink, and reprocessed on a Quarterly basis before delivery to MAST. The PAD attitude errors (RA, Dec, roll) for Q4 are shown in Figure 14. The maximum attitude residual (MAR) is the largest distance between the expected and actual location of a star in its aperture, for a given Cadence. The RSS sum of RA, Dec, and roll errors is an upper bound on the rigid body component of MAR and is also shown in the Figure.

Since continued attitude drift would invalidate target aperture definitions and lead to large photometric errors, small attitude adjustments (“tweaks”) are performed if necessary to ensure that MAR is always < 100 mpix. In Q2, tweaks were necessary, and they introduced discontinuities into the data which were not fully compensated by the initial version of the Pipeline. Parameter changes in the FGS centroiding algorithm, which were implemented at the start of Q3, have apparently greatly diminished the boresight drift.

There were no tweaks in Q4 since the drift did not grow to an unacceptable level.

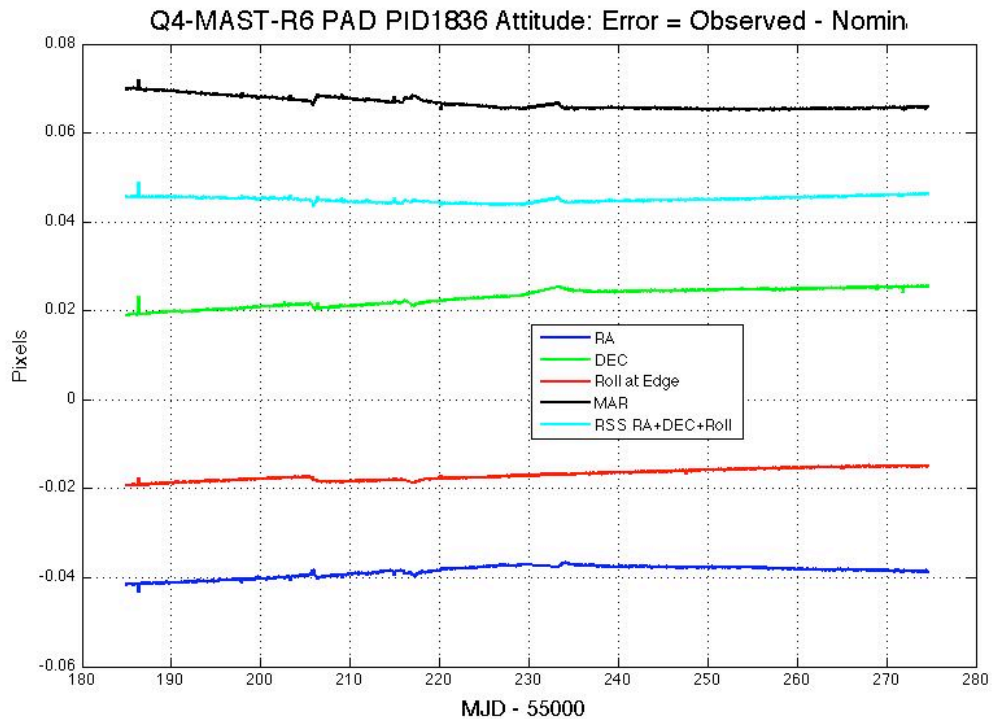


**Figure 14: Attitude Error in Quarter 4, calculated by PAD using Long Cadence data.**

### 5.3.4 Downlink Earth Point

Science data is downlinked once a month, and the spacecraft changes its attitude to point its fixed High Gain Antenna (HGA) at the Earth. Science data collection ceases, and the change in attitude induces a thermal transient in the Photometer. In this Release, data collected after Earth Point are corrected in the same way as data after a Safe Mode.

There was only one Earth Point in Q4, since the six weeks of data after the long Safe Mode were downlinked at the end of the Quarter.

### 5.3.5 Manually Excluded Cadences

Occasionally, a Cadence is manually excluded, usually near a gap or discontinuity in the data which makes it difficult to exclude them automatically. It was not necessary to do this in Q4 Release 6.

### 5.3.6 Anomaly Summary Table

Table 5 shows a summary of the Anomalies for both LC and SC data. COARSE\_POINT in the SC table indicates normal attitude recovery after a momentum dump and not a Loss of Fine Point event (Section 5.3.2).



**Table 5: Anomaly Summary Table for Long and Short Cadences.** The 'ATTITUDE\_TWEAK' at Long Cadence Index Number 12936 was used to alert the Pipeline to light curve features resulting from the failure of module 3 at LC CIN = 12935 and the consequent change of CCD and LDE temperatures; no actual attitude adjustment occurred at that time. The SC 'COARSE\_POINT' is subsequent to a momentum dump and does not represent a LOFP event.

LC CIN			MJD	
Start	End	Anomaly Type	Start	End
11983	11983	ARGABRIGHTENING	55186.2774	55186.2979
12936	12936	ATTITUDE_TWEAK	55205.7507	55205.7711
12967	12967	ARGABRIGHTENING	55206.3841	55206.4045
13337	13337	ARGABRIGHTENING	55213.9445	55213.9650
13434	13476	EARTH_POINT		
13642	13642	ARGABRIGHTENING	55220.1768	55220.1972
14091	14284	SAFE_MODE	55229.3515	55233.3156
14979	14979	ARGABRIGHTENING	55247.4965	55247.5169

SC CIN			MJD	
Month	Start	End	Start	End
Q4M1	347963	347963	55186.2863	55186.2870
Q4M1	377476	377476	55206.3882	55206.3889
Q4M1	388597	388598	55213.9629	55213.9643
Q4M1	391340	391353	55215.8312	55215.8401
Q4M1-M2	392770	392770		55216.8059
Q4M2	397748	397751	55220.1958	55220.1986
Q4M2	411190	416980	55229.3515	55233.3163
Q4M3	437838	437842	55247.5019	55247.5054

#### 5.4 Module 3 failure

All 4 outputs of Module 3 failed at 17:52 UTC Jan 9, 2010, during LC CIN 12935. Reference pixels showed loss of stars and black levels decreased by 75 to 100 DN per frame. FFIs show no evidence of photons or electrically injected signals. The start of line ringing and FGS crosstalk are still present after the anomaly (Figure 15).

The loss of the module led to consistent temperature drops within the LDE, telescope structure, Schmidt corrector, primary mirror, FPA modules, and acquisition/driver boards – which in turn affected photometry and centroids as shown in various Figures in these Notes.

After a review of probable causes, it was concluded that the probability of a subsequent failure was remote, a conclusion supported by continued operation of all the other Modules in the last 6 months.

The impact on science observations is that 20% of the FOV will suffer a one-Quarter data outage every year as Kepler performs its quarterly rolls.

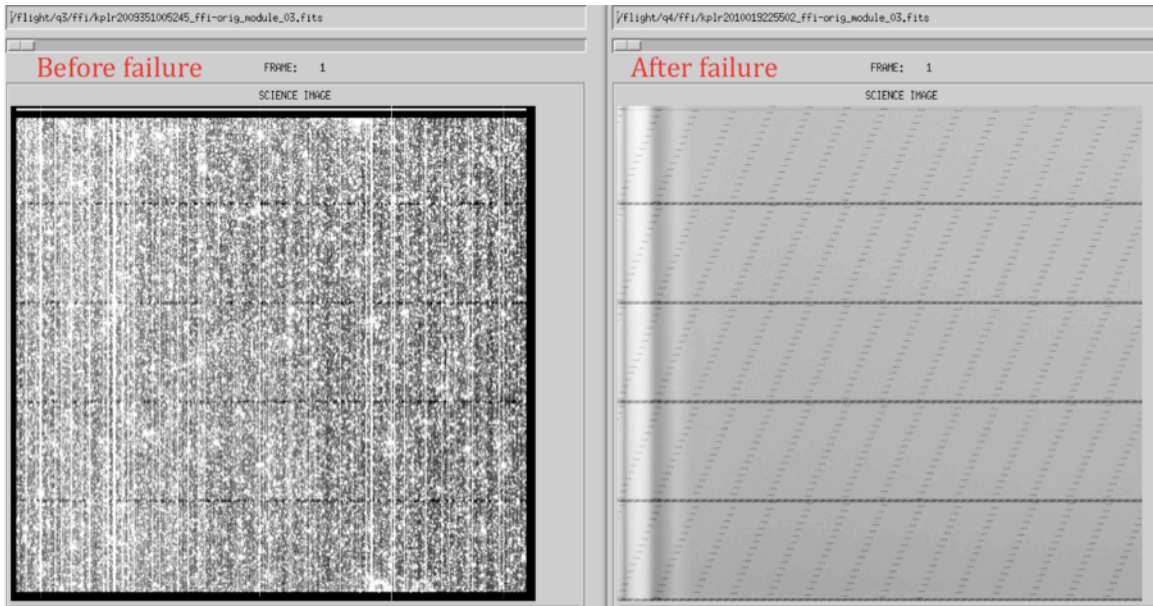


**Figure 15: Permanent loss of Module 3.** The left image is a normal uncalibrated FFI; the right is the image collected after the failure. Black-white image scaling is 1551 DN/cadence = 5.7 DN/frame for both images.

### **5.5 *Incomplete Apertures Give Flux and Feature Discontinuities at Quarter Boundaries***

While some mismatch of flux at Quarter boundaries is expected, since the target has moved to a different mod.out with a possibly different aperture and crowding metric, some users have reported larger than expected flux and flux slope discontinuities between Quarters. Even worse, changes in relative feature depths between Quarters have also been seen. In each case to date, the problem has been that the optimal aperture pixels (Ref. 16) have omitted bleeding charge from sources which saturate 3 or more pixels (Kepler magnitude 11 or brighter). The problem at the Quarter boundary can be substantially mitigated by summing all the calibrated pixels, not just those in the optimal aperture. However, if charge has bled outside the full target aperture (which includes a halo of pixels around the estimated optimal subset), then that information is irretrievably lost. Unfortunately, target pixel files are not yet available to users, so users concerned about large interQuarter discontinuities in bright star flux time series need to contact the Science Office.

The most important reasons for this problem are

- (1) Variability of sources, when that variability exceeds a few percent, since the optimal aperture is designed for a fixed Kepler magnitude.
- (2) Inability of the focal plane nonlinearity model to predict in detail the length and position of the charge bleed pixels in a column containing a saturating source. For example, a bright source may have 75% of the saturating pixels at lower rows, and 25% at higher, than the row on which the source is centered – while an equally bright source in another location on the same mod.out might have 50% above and 50% below, or even 25% below and 75% above. The saturation model currently in use can accommodate 25/75 to 75/25 asymmetries by collecting extra pixels along the saturating column, but larger asymmetries leave bleeding charge uncaptured.

As the mission progressed visual inspection revealed those stars with poorly captured saturation. The Kepler magnitudes of these stars were adjusted in subsequent quarters so that they were assigned larger apertures. Therefore more targets will have problems with incomplete apertures

early in the mission, though incomplete optimal aperture problems have been reported as late as Q3.

Two more general long-term fixes are being pursued:

- (1) For future quarters selecting apertures for both data acquisition and optimal apertures based upon actual flux distribution in exposures taken at the same roll previously.
- (2) Adopting some dynamic selection of pixels for optimal apertures in pipeline processing based on actual flux distribution.

## 6. Systematic Errors

This Section discusses systematic errors arising in on-orbit operations, most of which will be removed from flux time series by PA or PDC (Section 4). While the Release 6 data is cotrended against image motion (as represented by the Cadence-to-Cadence coefficients of the motion polynomials calculated by PA) as well as LDE board temperatures, other telemetry items which may be used for cotrending the data in future releases are included in the Supplement so that users can at least qualitatively assess whether features in the time series look suspiciously like features in the telemetry items. This telemetry has been filtered and gapped as described in the file headers, but the user may need to resample the data to match the LC or SC sampling. In addition, PDC corrects systematic effects only in the flux time series, and this Section and Supplement files may be useful for users interested in centroids or pixel data (when available).

Most of the events described in this Section are either reported by the spacecraft or detected in the Pipeline, then either corrected or marked as gaps. This Section reports events at lower thresholds than the Pipeline, which affect the light curves and therefore may be of interest to some users.

### 6.1 Argabrightening

*Argabrightening*, named after its discoverer, V. Argabright of BATC, is a presently unexplained diffuse illumination of the focal plane, lasting on the order of a few minutes. It is known to be light rather than an electronic offset since it appears in calibrated pixel data from which the electronic black level has been removed using the collateral data. It is not a result of gain change, or of targets moving in their apertures, since the phenomenon appears with the same amplitude in background pixels (in LC) or pixels outside the optimal aperture (in SC) as well as stellar target pixels. Many channels are affected simultaneously, and the amplitude of the event on each channel is many standard deviations above the trend, as shown in Figure 16.

The method of detection is

1. Calculate the median, for each Cadence and mod.out, of the calibrated background (LC) or out-of-optimal-aperture (SC) pixels,
2. Detrend the data by fitting a parabola to the resulting time series and subtract the fit.
3. High-pass filter the detrended data by median filtering the detrended data using a 25 Cadence wide filter, and subtracting that median-filtered curve from the detrended data to form the residual background light curve.
4. Calculate the Median Absolute Deviation (MAD) of the residual. The Argabrightening statistic  $S_{\text{Arg}}$  is then ratio of the residual to the MAD.
5. Find  $S_{\text{Arg}}$  which exceed the single-channel threshold  $T_{\text{MAD}}$ , and subsequently treat those Cadences as gaps for all pixels in that channel. In the current version of the Pipeline,  $T_{\text{MAD}}$  is the same for all channels.
6. A multichannel event is detected on a given Cadence if the number of mod.outs for which  $S_{\text{Arg}} > T_{\text{MAD}}$  on that Cadence exceeds the multi-channel event threshold  $T_{\text{mce}}$ . Then all mod.outs on that Cadence are marked as gaps, even those channels which did not individually exceed  $T_{\text{MAD}}$ . Multichannel event detection allows the use of lower  $T_{\text{MAD}}$  while still discriminating against spurious events on isolated channels.
7. For multichannel events, average  $S_{\text{Arg}}$  over all 84 outputs of the FPA to form  $\langle S_{\text{Arg}} \rangle_{\text{FPA}}$

The Pipeline uses a rather high  $T_{\text{MAD}} = 100$  for LC and 60 for SC, and a high  $T_{\text{mce}} = 42$  (half the mod.outs). While it appears that background subtraction has mostly removed this phenomenon from the delivered Long Cadence data, the residual effect has not been proven to be negligible in all cases, especially in Short Cadence data. There may also be significant Argabrightening events in both LC and SC, which do not exceed the thresholds. This Section gives a summary of

events with lower thresholds  $T_{MAD} = 10$  and  $T_{MCE} = 10$  (Table 6 and Table 7), so that the user may consider whether some Cadences of interest might be afflicted by Argabrightening, but not identified as such by the Pipeline and gapped (i.e., -Inf in all columns of the light curve file, except those referring to time or CIN). The Supplement contains these detection summaries as ASCII files.

The Supplement also contains the channel-by-channel background time series so users can identify low-level or few-channel Argabrightenings using their own criteria. These time series may also be useful for correcting SC data collected during Argabrightening events, since the Pipeline background correction interpolates LC background data to calculate the background for SC data. Users may notice some “chatter” in the background time series. A preliminary study shows that the problem is present in the calibrated background pixels, but not in the raw pixels, and is present in about 25% of the channels, with an amplitude up to 3% of the background. The reasons are still under investigation.

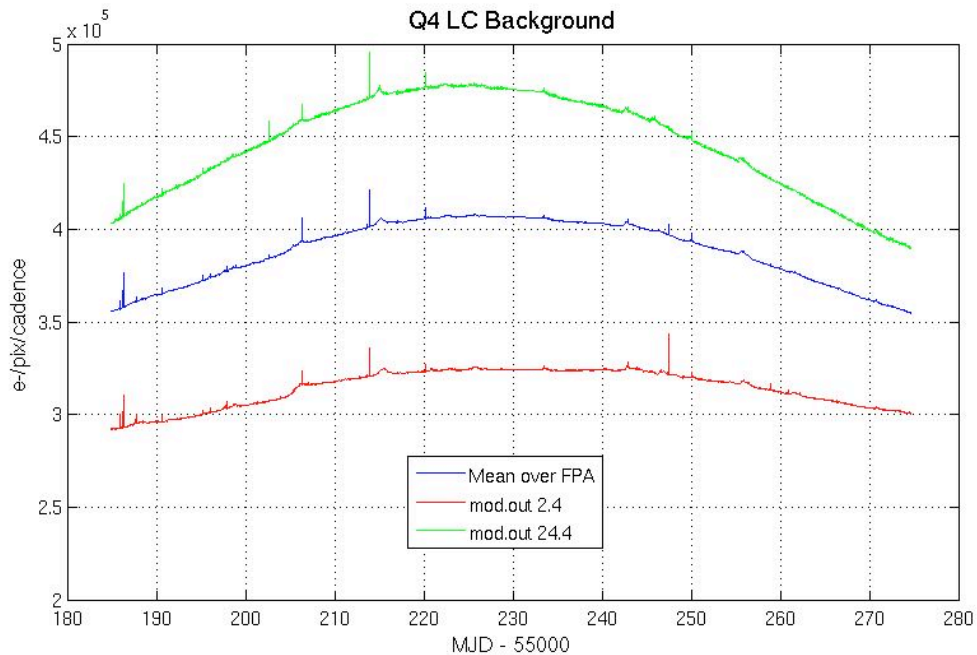


**Figure 16: Background time series for Q4 showing the average over all mod.outs, and the modules furthest from (2.4) and nearest to (24.4) the Galactic plane. The narrow spikes common to all 3 curves are Argabrightening events.**

**Table 6: Q4 LC Argabrightening Events with amplitude greater than 10x the median absolute deviation (MAD), which occurred simultaneously on at least 11 of the 84 channels. The columns are (1) CIN = Cadence Interval Number for Argabrightening Cadences, (2) RCI = Relative Cadence Index for Argabrightening Cadences, (3) Date = Arg Cadence mid-Times, MJD, (4) Mean Argabrightening statistic over Channels of Arg Event  $\langle S_{Arg} \rangle_{FPA}$  (5)  $N_{chan}$  = Channels exceeding threshold in Arg Cadence, (6)  $N_{pipe}$  = Channels exceeding default (Pipeline) threshold in ArgCadence. MAD is calculated on a channel-by-channel basis.**

**Q4**

11966	53	55185.94028	33.3	79	0
11983	70	55186.28765	145.7	80	62
12053	140	55187.71801	18.6	52	0
12194	281	55190.59914	28.2	77	0
12422	509	55195.25800	21.2	78	0
12463	550	55196.09578	15.9	59	0
12550	637	55197.87350	19.7	75	0
12605	692	55198.99735	11.5	41	0
12783	870	55202.63453	17.2	22	3
12918	1005	55205.39307	6.7	15	0
12967	1054	55206.39431	97.1	80	33
13278	1365	55212.74916	6.6	13	0
13321	1408	55213.62781	12.4	45	0
13337	1424	55213.95475	151.7	80	72
13395	1482	55215.13989	4.2	11	0
13396	1483	55215.16033	4.4	13	0
13400	1487	55215.24206	3.8	14	0
13402	1489	55215.28293	4.3	11	0
13403	1490	55215.30336	3.1	11	0
13404	1491	55215.32380	3.2	12	0
13405	1492	55215.34423	3.2	11	0
13406	1493	55215.36466	3.0	14	0
13407	1494	55215.38510	3.0	12	0
13490	1577	55217.08109	8.6	29	0
13642	1729	55220.18699	45.6	80	4
13643	1730	55220.20743	4.7	11	0
14293	2380	55233.48927	10.6	46	0
14749	2836	55242.80699	5.3	13	0
14755	2842	55242.92959	15.6	58	0
14979	3066	55247.50672	40.7	73	3
15103	3190	55250.04048	27.3	77	0
15390	3477	55255.90493	7.4	19	0
15536	3623	55258.88823	6.6	13	0
15637	3724	55260.95203	6.7	21	0

**Table 7: Same analysis as Table 6, for Q4 SC. Note consecutive detections of the largest events. A horizontal line separates the 3 Months of the Quarter. The relative cadence index (RCI) is reset at the start of each Month.**

**Q4**

CIN	RCI	Date (MJD)	MeanSNR	N <sub>chan</sub>	N <sub>pipe</sub>
347458	1579	55185.94267	25.8	80	0
347459	1580	55185.94335	9.1	30	0
347963	2084	55186.28663	142.1	80	80
347964	2085	55186.28731	4.6	11	0
350071	4192	55187.72243	11.0	38	0
354291	8412	55190.59676	27.7	80	0
361142	15263	55195.26311	21.2	80	0
362362	16483	55196.09408	13.0	58	0
364977	19098	55197.87521	19.9	76	0
366635	20756	55199.00450	11.8	50	0
377476	31597	55206.38852	94.3	79	68
386824	40945	55212.75563	6.7	11	0
388597	42718	55213.96326	136.6	80	80
388598	42719	55213.96394	16.2	66	0
391351	45472	55215.83906	6.0	12	2
-----					
393189	420	55217.09096	9.1	25	0
397748	4979	55220.19619	42.3	79	6
397749	4980	55220.19687	3.5	11	0
417255	24486	55233.48280	7.5	12	0
431117	38348	55242.92448	13.9	60	0
-----					
437838	2499	55247.50229	29.6	69	7
437839	2500	55247.50297	7.2	13	1
441550	6211	55250.03061	27.6	78	0
457577	22238	55260.94692	6.5	20	0

## 6.2 Variable FGS Guide Stars

Variable FGS Guide stars are not expected to be significant in Q4 photometry.

## 6.3 Pixel Sensitivity Dropouts

*Section 6.3.1 is unchanged from Release 4, where it was labeled Section 6.3. Section 6.3.2 is entirely new.*

### 6.3.1 Particle-induced

*This Section is unchanged from Release 4.*

Space-based focal planes respond to cosmic ray (CR) events in several ways:

1. A transient response is induced by the charge deposited by the CR, and is cleared by the next reset (destructive readout) of the pixel.
2. Medium-term alteration of detector properties, which recover to near or at their pre-event values after some time and resets without annealing.
3. Long-term alteration of detector properties, which are only restored by annealing the focal plane
4. Permanent damage

Typically, type 3 and 4 effects are caused by non-ionizing energy loss (NIEL), or “knock-on” damage, which can be caused by any baryonic particle.

Type 1 effects are removed by the Pipeline’s CR detection algorithm. At this point in the mission, type 3 effects do not appear to be common enough to warrant the disruption of the observing schedule that would be caused by annealing, and both type 3 and type 4 effects will eventually be mitigated by updating the bad pixel map used for calibration. Type 2 effects are not corrected by the Pipeline at the pixel level (Figure 17). In this Release, the Pipeline corrects the aperture flux discontinuities (Figure 18) resulting from these pixel discontinuities (Section 4.4), though users examining pixel data and uncorrected light curves need to remain aware of them.

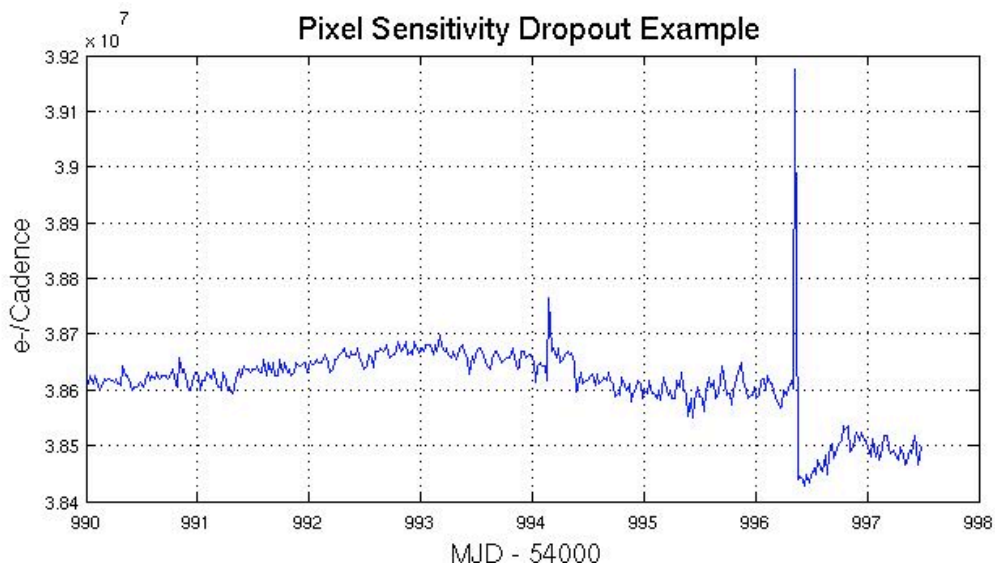


**Figure 17: Pixel time series from Q1 (Release 2) showing discontinuity after large CR event. CRs have not been removed by the Pipeline at this stage of processing. Target: KeplerID = 7960363, KeplerMag = 13.3. Dropouts are not corrected on a pixel-by-pixel basis.**



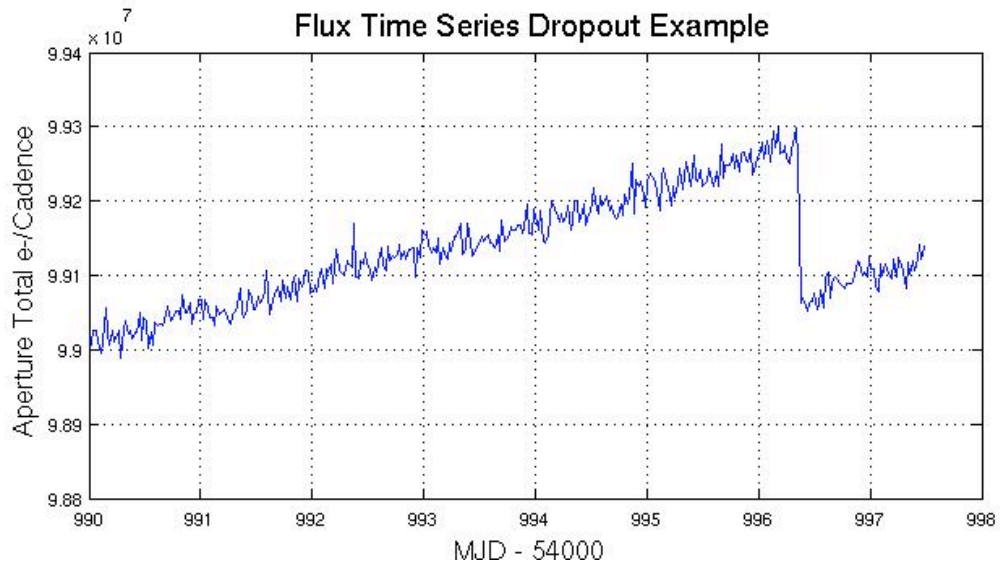


**Figure 18:** Same event as for the previous Figure as seen in the uncorrected Simple Aperture Photometry (SAP) light curve produced by PA. CR hits have been removed by PA. This figure is presented for historical interest, as PDC identifies most of these discontinuities and removes them before producing the corrected light curves (Section 4.4).

### 6.3.2 Mod.out 4.2 performance discontinuity

Mod.out 4.2 shows step changes in behavior during Q4M1. These changes manifest as gain/linearity changes and noise level changes. The first such change occurred on Jan 6, approximately 86 hours before the module 3 failure. The second change occurred coincident with the temperature change at the module 3 failure, but does not appear to be a simple temperature dependent black-level change. The effect is most prominent at lower row numbers. The effect on read noise and other detector properties, and the influence on other module 4 outputs suggests a non-thermally-driven change in a physical parameter of some channel 4.2 circuit element.

No significant changes in any other modules at the time of the first step were seen, except that all other module 4 outputs have low-level step changes in collateral signals possibly caused by some form of cross-talk from 4.2. The direct effect of the observed behaviors on science is small since it only affects a small fraction (<30%) of one channel.

This discontinuity on mod.out 4.2 is still under investigation by the Science Office.

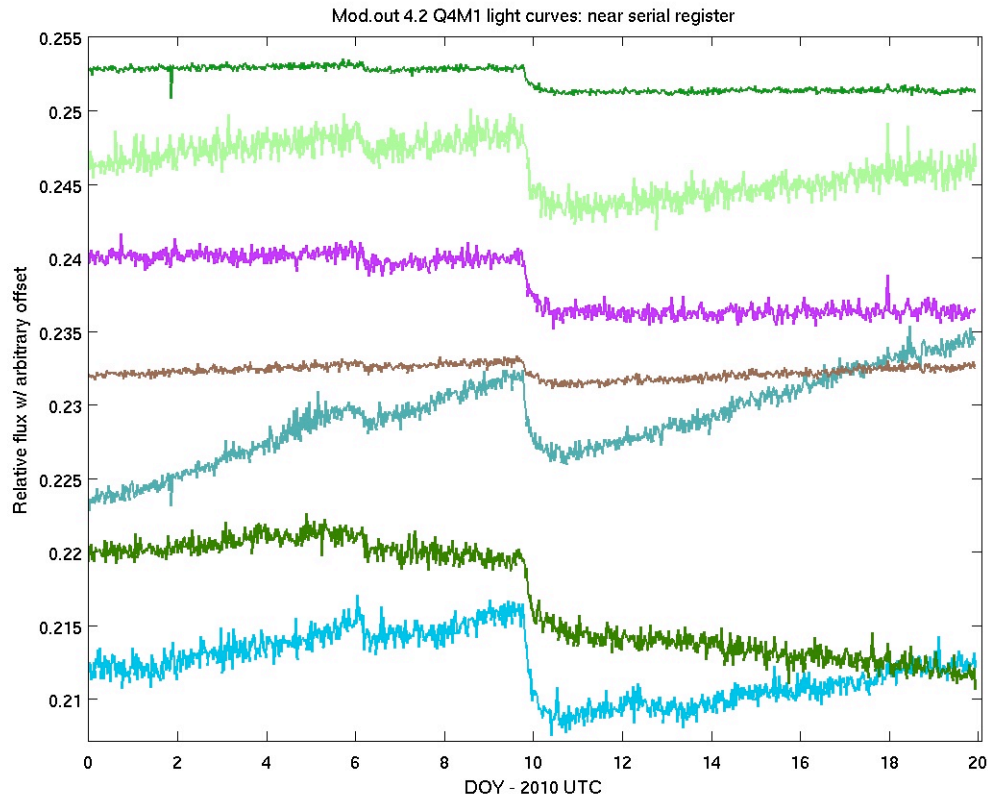


**Figure 19: Sample uncorrected light curves that clearly show the step in mod.out 4.2 performance near Day of Year (DOY) 6 and the effect of the failure of mod 3 near DOY 9.7. These targets are selected from low CCD row numbers**

#### **6.4 Focus Drift and Jitter.**

Examination of Q1 data (Figure 20) revealed that many of the science targets exhibit non-sinusoidal variations in their pixel time series with a period between 3 and 6 hours. The behavior was less frequent at the beginning of Q1 and becomes progressively worse with time. Initially, this phenomenon was associated with desaturation activities, but became nearly continuous about 15 days into the observations. The problem persisted through the end of Q3 (see Release 4 Notes, KSCI-19044).

This jitter was observed in platescale metrics local to each mod.out defined by the motion of target star centroids relative to one another over time. This indicated a change in focus at timescales of 3 to 6 hours and that the behavior was initiated by the desat activities. Reaction wheel temperature sensors with the mnemonics TH1RW3T and TH1RW4T had the same time signature, but the physical mechanism by which they coupled to focus is still under discussion. At the beginning of Quarters 1-3, the reaction wheel heaters did not cycle on and off, and the temperature changes have the same 3 day interval as the planned desaturations. Later in these Quarter, the heaters cycled with a 3 to 6 hr period. Near the end of Q3, at MJD = 55170, new Flight Software parameters were uploaded to substantially reduce the deadband on the reaction wheel housing temperature controller, and subsequent to that date the 3 to 6 hr cycle in both the temperature telemetry and the focus metric were eliminated, leaving only a slow seasonal drift and the 3 day signature of the momentum management cycle (Figure 21).

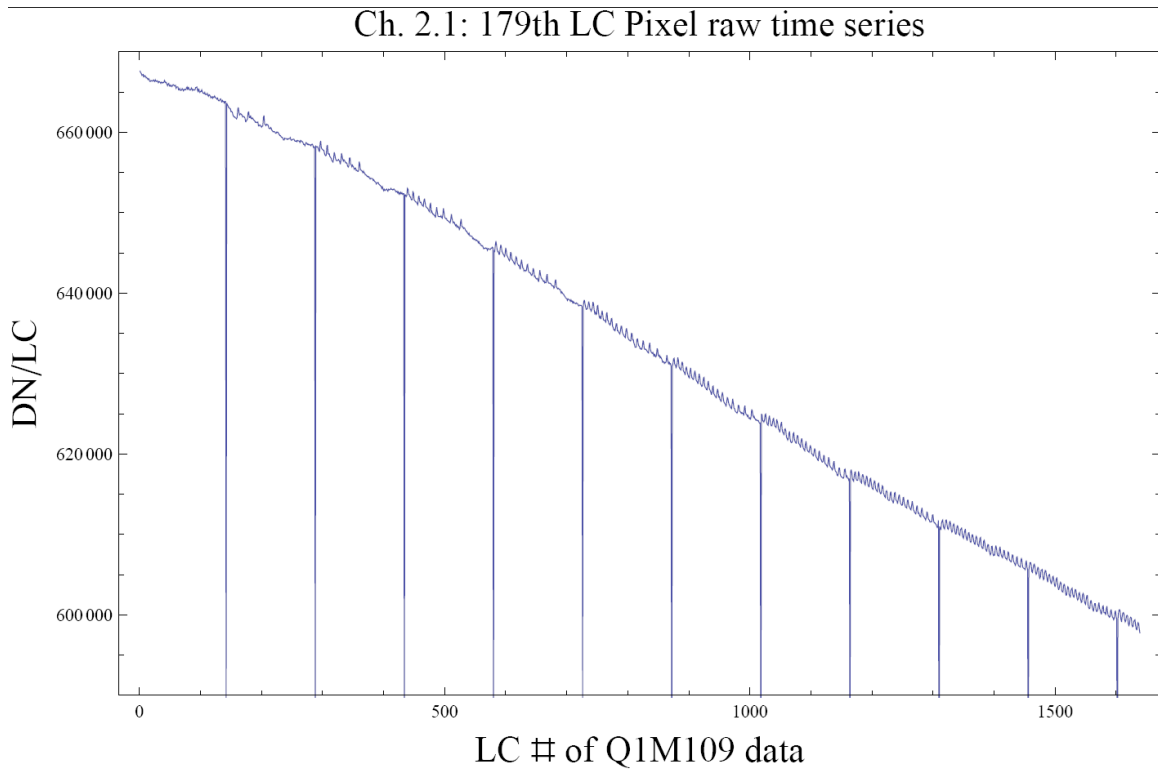


**Figure 20: A good example of the 3 to 6 hr Focus Oscillation in a single raw pixel time series from Quarter 1. Similar signatures are seen in flux and plate scale. The large negative-going spikes are caused by desaturations (Section 5.1), which have not been removed from this time series in this plot. The abscissa is the Q1 relative Cadence index, and the ordinate is Data Numbers (DN) per Long Cadence (LC).**

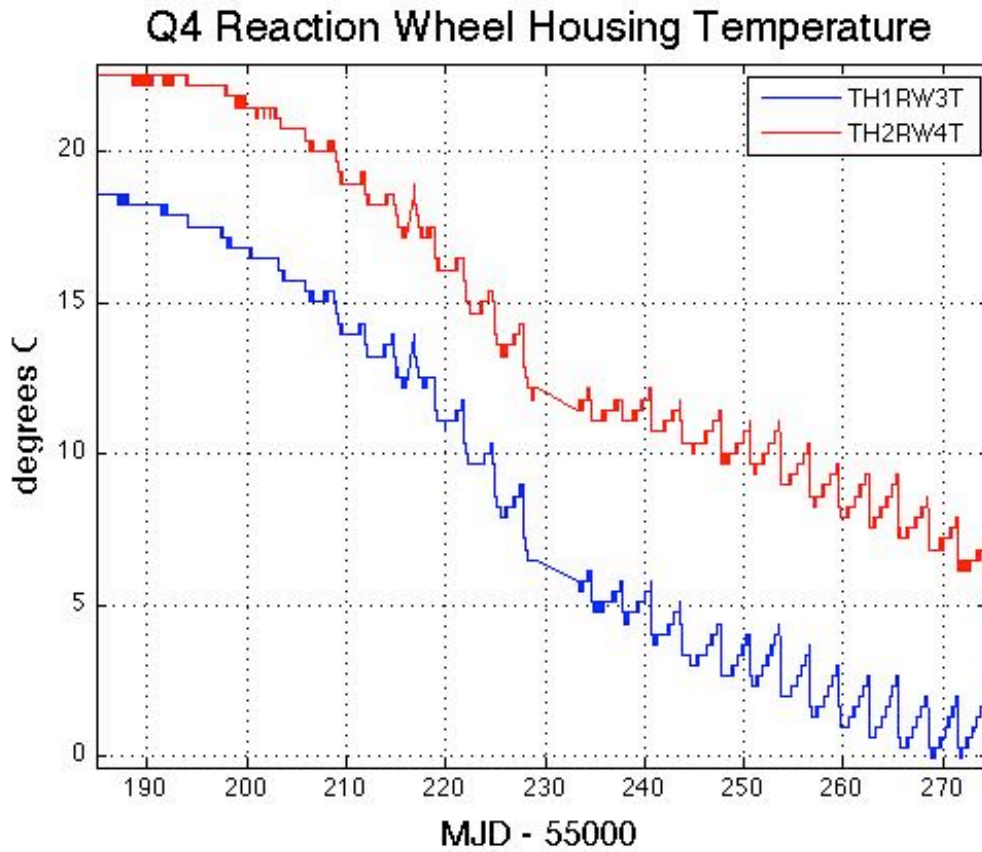


**Figure 21: Reaction wheel housing temperatures during Q4. Temperature variation in Q4 is dominated by a slow seasonal drift and the 3 day period of reaction wheel desaturations. The telemetry data in this Figure is not plotted for times when the spacecraft is not in Fine Point, and is smoothed with a 5 point median filter.**

The DAWG investigated whether there is a secular variation of the focus and PRF width driven by the outgassing of telescope components, in addition to the seasonal and momentum dump cycles driven by temperature changes in Flight System components discussed above. Preliminary results indicate that the seasonal cycle dominates, with a good correlation between PRF width variation and the temperature of the Launch Vehicle Adapter (TH2LVAT), as shown in Figure 22. The pattern has begun to repeat, now that a full year of science data collection has passed.

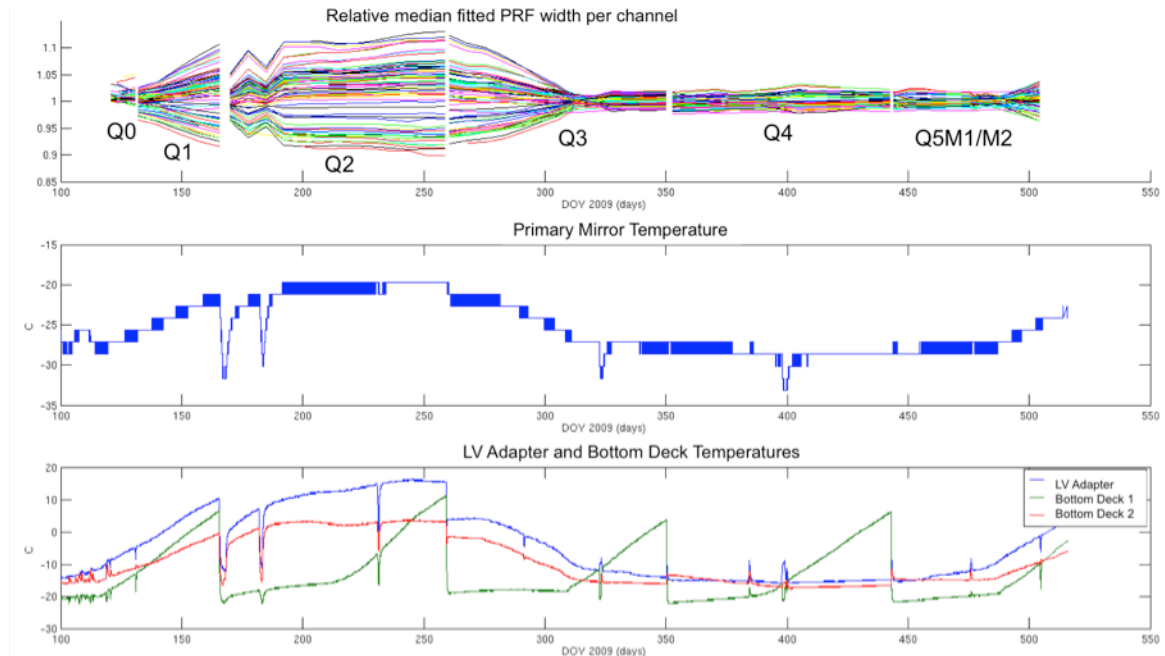


**Figure 22: Correlation of variation in PRF width with various spacecraft temperatures, demonstrating the seasonal nature of focus and PRF changes.**

For users of the PDC output, the focus changes are mostly captured by the motion polynomial coefficients used for cotrending. For users doing their own cotrending, the mod.out center motion time series provided in the Supplement will represent much of the image motion resulting from focus changes, for all targets on the corresponding mod.out. However, they do not represent local plate scale changes, which may contribute systematic errors to the light curves of individual targets on that mod.out. Thus the reaction wheel and Launch Vehicle Adapter temperature sensor telemetry for Q4 are also provided in the Supplement.

### 6.5 Short Cadence Requantization Gaps

*This section is unchanged since Release 4, except to emphasize this is a Short Cadence phenomenon.*

Short Cadence pixels at mean intensities  $>20,000$  e<sup>-</sup> show banding as shown in Figure 23, with quantized values of number of electrons preferred. This is the result of the onboard requantization (KIH Section 7.4), and is considered benign since in the overall extraction the light curve is near the Poisson limit. These requantization gaps are expected, and a necessary cost associated with achieving the required compression rates on board Kepler. However, it is pointed out here so that users will not suspect a problem.

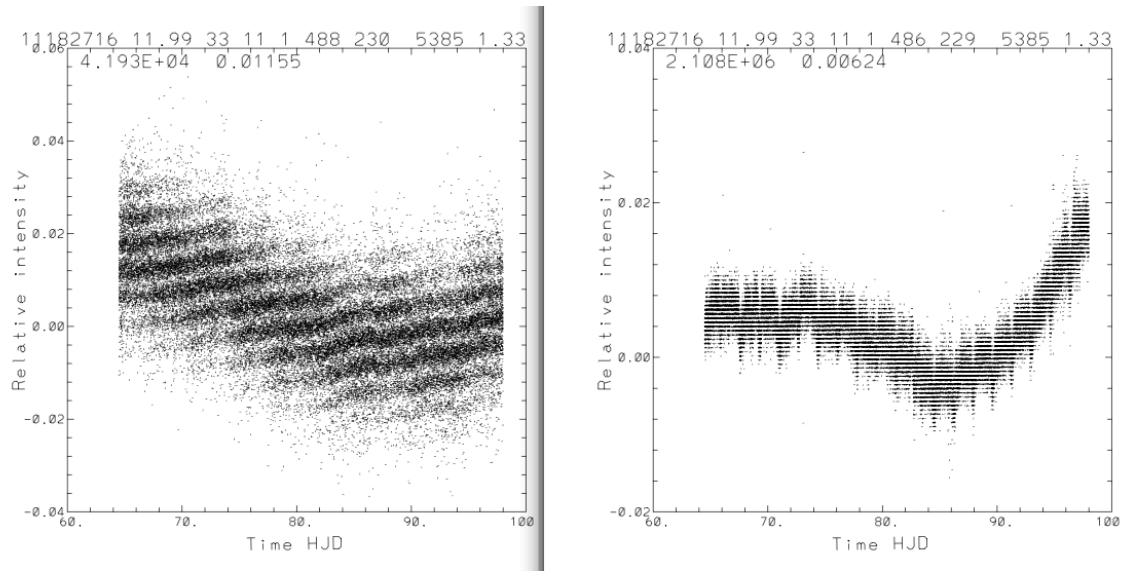


**Figure 23: Requantization gap example in Q1 SC pixel time series. The ‘band gaps’ scale with mean intensity (42,000 e- left, 2.1e6 right). See KIH Section 7.4 for a discussion of quantization and the (insignificant) information loss it entails.**

## 6.6 Spurious Frequencies in SC Data

*Section 6.6.1 is unchanged from Releases 4-5, where it was labeled Section 6.6. Section 6.6.2 is entirely new.*

### 6.6.1 Integer Multiples of Inverse LC Period

Spurious frequencies are seen in SC flux time series, and pixel data of all types – including trailing black collateral pixels. The frequencies have an exact spacing of  $1/\text{LC}$  interval, as shown in Figure 24. As the SC data are analyzed in the frequency domain in order to measure the size and age of bright planetary host stars, the contamination of the data by these spurious frequencies will complicate these asteroseismology analyses, but will not compromise the core Kepler science. The physical cause of this problem is still under discussion, though the problem might be remedied with a simple comb notch filter in future releases even if no ancillary data can be found that exhibits these features.

This feature was first reported in Q1 data (Ref. 8). It has now been identified in pre-launch ground test data as well as Q3 flight data, and is therefore considered a normal feature of the as-built electronics. It is not an artifact introduced by the Pipeline, since it appears in raw trailing black collateral data.

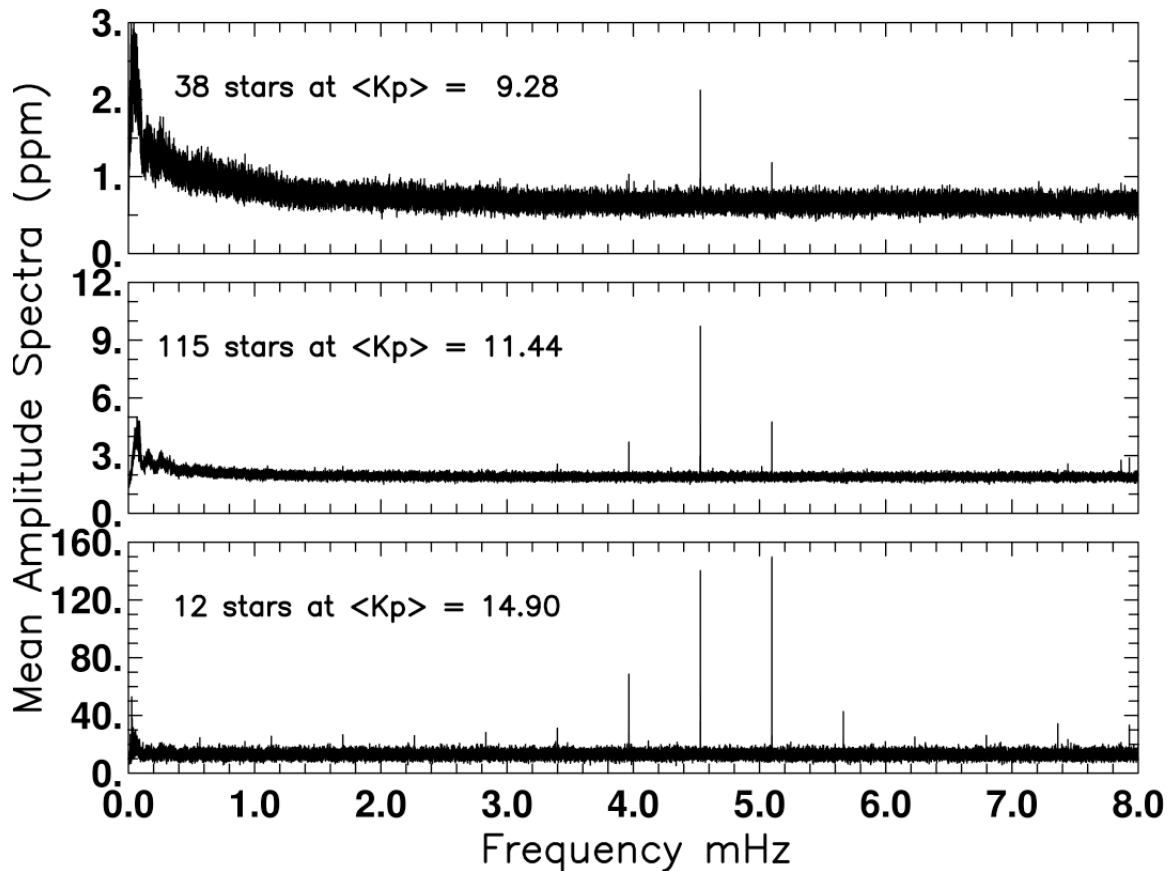


**Figure 24: Mean amplitude spectra over samples of quiet stars from Q1, spanning more than a factor of 100 in brightness, showing spurious frequencies. The 1/LC-Cadence artifacts at the fundamental of 0.566391 mHz and all harmonics are visible for the faint star set in the bottom panel. Even at 9th magnitude in the upper panel this artifact remains a dominant spectral feature from the 7th and 8th harmonics. From Gilliland et al. (Ref. 8).**

### 6.6.2 Other Frequencies

Further analysis of SC data in Q1 and subsequent Quarters showed several stars in which the SC data showed peak power at 7865  $\mu\text{Hz}$  ( $\sim 127.16$  seconds). This is not a harmonic of the 1/LC noise discussed in the previous Section. Across the Q2M1 safing event, the phase shifted for both the 1/LC harmonics and for the 7865  $\mu\text{Hz}$  feature. Across the Q2M3 safing event the phase remained fixed. Since stellar signals tend to stay at the same phase, the phase shift across Q2M1 is evidence that the n/LC and 7865  $\mu\text{Hz}$  features are instrumental. Peaks have also been reported at 7024, 7444, 7865, and 8286  $\mu\text{Hz}$  -- consistent with a splitting of 421  $\mu\text{Hz} = 2375.3$  s, or 39.59 minutes.

In Q0-Q2, multiple groups reported the issues around 80-95  $\mu\text{Hz}$  which correspond to about 3.2 hours. The non-sinusoidal nature of these spurious signals leads to evenly spaced peaks, not unlike stellar oscillations. Since this is the same period as the temperature variation of the reaction wheel housing temperature, and that variation has been eliminated by reducing the corresponding temperature controller deadband, 3.2 hr features should be undetectable in Q4 (Section 6.4). Users are, however, encouraged to examine the thermal telemetry shown in these Notes and provided in the Supplement to strengthen the case that detected spectral features are astrophysical not instrumental.

In Q3, broadband features around 270 - 360  $\mu\text{Hz}$  occur in several stars, corresponding to periods of 0.75 - 1 hour.

Q4 SC data has not yet been characterized for potential unique behavior.

A period of about 3 days has been reported multiple times, and is almost certainly associated with the momentum management cycle and associated temperatures (Figure 21).

**Table 8: List of Possible Spurious Frequencies in SC data. Users are advised to check detections against this list, and report additional spurious frequencies to the Science Office. Labels: RW = reaction wheel passive thermal cycle associated with momentum cycle. RWTH = Reaction wheel housing temperature controller thermal cycling (believed not to be a problem from Q3 onward). U = unknown. Narrow lines are defined as  $\nu/\Delta\nu > 50$ , broad lines as  $\nu/\Delta\nu < 50$ .**

**SC spurious frequency summary**

frequency uHz	frequency $\text{d}^{-1}$	period S	period min	period hr	period d	Label	width
8.9	0.33	112320.00	1872.000	72.0000	3.00000	RW	?
86.8	7.50	11520.00	192.000	3.2000	0.13333	RWTH	broad
290.0	25.06	3448.28	57.471	0.9579	0.03991	U1	broad
340.0	29.38	2941.18	49.020	0.8170	0.03404	U2	broad
360.0	31.10	2777.78	46.296	0.7716	0.03215	U3	narrow
370.4	32.00	2700.00	45.000	0.7500	0.03125	U4	narrow
421.0	36.37	2375.30	39.588	0.6598	0.02749	splittingU5- U8	narrow
566.4	48.94	1765.56	29.426	0.4904	0.02043	1/LC	narrow
1132.8	97.87	882.78	14.713	0.2452	0.01022	2/LC	narrow
1699.2	146.81	588.52	9.809	0.1635	0.00681	3/LC	narrow
2265.6	195.74	441.39	7.357	0.1226	0.00511	4/LC	narrow
2832.0	244.68	353.11	5.885	0.0981	0.00409	5/LC	narrow
3398.3	293.62	294.26	4.904	0.0817	0.00341	6/LC	narrow
3964.7	342.55	252.22	4.204	0.0701	0.00292	7/LC	narrow
4531.1	391.49	220.70	3.678	0.0613	0.00255	8/LC	narrow
5097.5	440.43	196.17	3.270	0.0545	0.00227	9/LC	narrow
5663.9	489.36	176.56	2.943	0.0490	0.00204	10/LC	narrow
6230.3	538.30	160.51	2.675	0.0446	0.00186	11/LC	narrow
6796.7	587.23	147.13	2.452	0.0409	0.00170	12/LC	narrow
7024.0	606.87	142.37	2.373	0.0395	0.00165	U5	narrow
7363.1	636.17	135.81	2.264	0.0377	0.00157	13/LC	narrow
7444.0	643.16	134.34	2.239	0.0373	0.00155	U6	narrow
7865.0	679.54	127.15	2.119	0.0353	0.00147	U7	narrow
7929.5	685.11	126.11	2.102	0.0350	0.00146	14/LC	narrow
8286.0	715.91	120.69	2.011	0.0335	0.00140	U8	narrow
8495.9	734.04	117.70	1.962	0.0327	0.00136	15/LC	narrow



### **6.7 *Known Erroneous FITS header keywords***

The automatically generated FFI WCS FITS header keyword values are known to be incorrect. However, starting with Release 6, FFIs will have corrected WCS header keywords as described in Section 7.1.

The WCS keywords in the light curve and target pixel file headers remain incorrect. However, the MODULE and OUTPUT keyword values are correct, and the row and column centroids values are in the files, so it is an easy matter to find the location of an observed target in an FFI to see the surrounding area. These keywords will be corrected when and if the recommendations described in Section 7.5 are implemented.

## 7. Data Delivered – Format

### 7.1 FFI

The FFIs are one FITS file per image, with 84 extensions, one for each module/output. See the KIH to map the extension table number = channel number onto module and output.

The Guest Observer office has developed a temporary procedure to populate FFIs with linear WCS information. Tests indicate that their solution is identical within 0.3 arcsec to the WCS coordinates computed by MAST staff using the public on-line astrometry.net tool (see the file WCSREADME.txt on the MAST FFI ftp site: <http://archive.stsci.edu/pub/kepler/ffi> ). The procedure provides a linear WCS solution, so distortion and DVA will cause systematic errors of  $\sim$  1.5 pixels in the corners of the FFI. The FFIs delivered in this Release will have these corrected WCS headers.

In the future Releases, FFIs will use the SIP convention for representing distortion in FITS image headers ([fits.gsfc.nasa.gov/registry/sip/SIP\\_distortion\\_v1\\_0.pdf](http://fits.gsfc.nasa.gov/registry/sip/SIP_distortion_v1_0.pdf)).

### 7.2 Light Curves

*This Section is unchanged since Release 4.*

Light curves have file names like kplr<kepler\_id>-<stop\_time>, with a suffix of either llc (Long Cadence) or slc (Short Cadence), and a file name extension of fits.

A light curve is time series data, that is, a series of data points in time. Each data point corresponds to a measurement from a Cadence. For each data point, the flux value from simple aperture photometry (SAP) is given, along with the associated uncertainty. Only SAP light curves are available at this time. The centroid position for the target and time of the data point are also included.

The light curves are packaged as FITS binary table files. The fields of the binary table, all of which are scalar, are briefly described below and are listed in Table 9. There are 19 fields comprising 88 bytes per Cadence; however, fields 12-19 are not populated at this time. The FITS table header listed in the Appendix of the MAST manual is superseded by Table 9. The new keywords `DATA_REL` and `QUARTER` discussed in Section 2 are in the binary table header. The module and output are identified in the binary table extension header keywords `MODULE` and `OUTPUT`.

The following data values are given for each data point in a light curve:

- barycentric time and time correction for the midpoint of the Cadence
- for the simple aperture photometry (pixel sum) of optimal aperture pixels
  - first-moment centroid position of the target and uncertainty
  - uncorrected flux value and uncertainty. Gap Cadences are set to -Inf
  - corrected flux value and uncertainty. Gap Cadences are set to -Inf

**Table 9: Available light curve data table fields, modified after the MAST manual KDMC-10008 (August 30, 2009): SAP replaces OAP, and data in columns 12-19 is not available and are filled with -Inf. Time units are the same as in Releases 3-5.**

Column Number	Field Name	Data Type	Bytes	Description	Units
1	barytime	1D	8	barycentric time BJD – 2400000. See Section 7.4 for detailed discussion.	days
2	timcorr	1E	4	barycentric time correction. See Section 7.4 for detailed discussion	seconds

Column Number	Field Name	Data Type	Bytes	Description	Units
3	Cadence_number	1J	4	Cadence number (CIN)	N/A
4	ap_cent_row	1D	8	row pixel location	pixels
5	ap_cent_r_err	1E	4	error in row pixel location	pixels
6	ap_cent_col	1D	8	column pixel location	Pixels
7	ap_cent_c_err	1E	4	error in column pixel location	pixels
8	ap_raw_flux	1E	4	SAP uncorrected flux	e- / Cadence
9	ap_raw_err	1E	4	SAP uncorrected flux error	e- / Cadence
10	ap_corr_flux	1E	4	SAP corrected un-filled flux	e- / Cadence
11	ap_corr_err	1E	4	SAP corrected un-filled flux error	e- / Cadence

#### Data Types:

1D – double precision floating point.

1E – single precision floating point. Note that, although all SOC calculations and internal data representation are double-precision, the SAP fluxes and errors are reported as single-precision floats, which will give roundoff errors of approximately 0.11 ppm (*Numerical Recipes* Chapter 20 & confirmed by numerical experiments on MAST and internal SOC data).

1J – 32 bit integer

See Section 7.4 for a discussion of time and time stamps.

If you are an IDL user, the `tbget` program in the `astrolib` library extracts the data. If you are an IRAF user, `tprint` can be used to dump an ascii table of selected row and column values.

### 7.3 Pixels

*This Section is unchanged since Release 4.*

Target **pixel** data files contain all the pixels for a target from all Cadences, while target **Cadence** files contain pixels from all targets for a single Cadence. Up to 5 different files are produced for each target. These consist of the Long and Short Cadence pixel data for the target, the collateral pixels for the Long and Short Cadences, and the background pixels.

Both original pixel values and calibrated flux values are in the pixel data files. The original pixel value is the integer value as recorded on the spacecraft. The calibrated pixel value is that provided by the SOC, and is equal to the output of CAL with cosmic rays removed. The calibrated pixels have **not** had background subtracted. Unfortunately, since the background is not subtracted, and users are not presently provided with the list of pixels in the optimal aperture, there is no simple way to construct the uncorrected (PA output) light curve from the ‘calibrated’ pixels. Users should be aware that the format and content of the target pixel files is the subject of vigorous discussion (Section 7.5), in the hopes of remedying this situation.

The target pixel data files are archived as a dataset. A request for the data will return all extensions that were archived with the dataset.

Pixel data table fields are described in the Kepler Archive Manual (KDMC-10008).

*Target Pixel Data Files are not currently available, but will be in the near future.*

## 7.4 Time and Time Stamps

The primary time stamps available for each Cadence in both LC and SC time series are intended to provide proper BJD times corrected to the solar system barycenter, at the flux-weighted mid-point of the Cadences, and are uniquely determined for each star individually.

*Users are urged to read this Section if they have not previously read the Releases 4 or 5 Notes, as a close reading may help them avoid attempting to do follow-up observations at the wrong time.*

### 7.4.1 Overview

*This Section is unchanged since Release 4.*

The precision and accuracy of the time assigned to a Cadence are limited by the intrinsic precision and accuracy of the hardware and the promptness and reproducibility of the flight software time-stamping process. The Flight System requirement, including both hardware and software contributions, is that the absolute time of the start and end of each Cadence is known to  $\pm 50$  ms. This requirement was developed so that knowledge of astrophysical event times would be limited by the characteristics of the event, rather than the characteristics of the flight system, even for high SNR events.

Several factors must be accounted for before approaching the 50 ms limit:

1. Relate readout time of a pixel to Vehicle Time Code (VTC) recorded for that pixel and Cadence in the SSR. The VTC stamp of a Cadence is created within 4 ms after the last pixel of the last frame of the last time slice of that Cadence is read out from the LDE.
2. VTC to UTC of end of Cadence, using information provided by the MOC to the DMC to convert between three time systems: 1) vehicle time code (VTC); 2) JPL Ephemeris Time (ET); and 3) Coordinated Universal Time (UTC). These conversions require leap second information and the spacecraft clock correlation.
3. Done by MOC, with precision and accuracy to be documented.
4. Convert UTC to Barycentric JD. This is done in PA (Section 4.3) on a target-by-target basis. The amplitude of the barycentric correction is approximately  $(a_K/c)\cos\beta$ , where  $a_K \sim 1.02$  AU is the semi-major axis of Kepler's approximately circular ( $e_K < 0.04$ ) orbit around the Sun,  $c$  the speed of light, and  $\beta$  is the ecliptic latitude of the target. In the case of the center of the Kepler FOV, with  $\beta = 65$  degrees, the amplitude of the UTC to barycentric correction is approximately  $\pm 211$  s. BJD is later than UTC when Kepler is on the half of its orbit closest to Cygnus (roughly May 1 – Nov 1) and earlier than UTC on the other half of the orbit. This correction is done on a target-by-target basis to support Kepler's 50 ms timing accuracy requirement.
5. Subtract readout time slice offsets (See KIH Section 5.1). This is done in PA (Section 4.3). The magnitude of the time slice offset is  $t_{rts} = 0.25 + 0.62(5 - n_{\text{slice}})$  s, where  $n_{\text{slice}}$  is the time slice index (1-5) as described in the KIH. Note that this will in general be different from Quarter to Quarter for the same star, as the star will be on different mod.outs, so the relative timing of events across Quarter boundaries must take this into account.

### 7.4.2 Time Stamp Definitions

*This Section is unchanged since Release 4.*

Cadence files:

JD = Julian Date

MJD = Modified Julian Date

MJD = JD - 2400000.5

1.  $\text{STARTTIME}(i) = \text{MJD of start of } i^{\text{th}} \text{ Cadence}$
2.  $\text{END\_TIME} = \text{MJD of end of } i^{\text{th}} \text{ Cadence}$
3.  $\text{MID\_TIME}(i) = \text{MJD of middle of Cadence} = (\text{STARTTIME}(i) + \text{END\_TIME}(i)) / 2$
4.  $\text{JD}(i) = \text{MID\_TIME}(i) + 2400000.5$

Releases 4-6 light curves, with barycentric and time slice corrections:

1.  $\text{timcorr}(i) = \text{dtB}(i) - t_{\text{rts}}$ , where  $\text{dtB}(i)$  = barycentric correction generated by PA, a function of Cadence  $\text{MID\_TIME}(i)$  and target position, and  $t_{\text{rts}}$  is the readout time slice offset described in Section 7.4.1. Units: seconds.
2.  $\text{BJD}(i) = \text{barycentric Julian Date} = \text{timcorr}(i) / 86400 + \text{JD}(i)$ . Units: days
3.  $\text{barytime}(i) = \text{Barycentric Reduced Julian Date} = \text{BJD}(i) - 2400000 = \text{timcorr}(i) / 86400 + \text{MID\_TIME}(i) + 0.5$ . Units: days
4.  $\text{LC\_START} = \text{MJD of beginning of first Cadence (uncorrected)}$ . Units: days
5.  $\text{LC\_END} = \text{MJD of end of last Cadence (uncorrected)}$ . Units: days

Or, as is summarized in the FITS table header:

`COMMENT barytime(i)- timcorr(i)/86400 - 0.5 = utc mjd(i) for cadence_number(i)`

Where `utc mjd(i) for cadence_number(i)` is the same as  $\text{MID\_TIME}(i)$

The difference between Release 3 and Releases 4-6

In Release 3,  $t_{\text{rts}} = 0$  for all targets, while in Release 4  $t_{\text{rts}}$  is calculated as described in Section 7.4.1. That is the only difference.

The vexing matter of the 0.5 days

Users should note that `barytime` follows the same conventions as Julian Date, and astronomers in general; that is, the day begins at noon. MJD, on the other hand, follows the convention of the civil world: that the day begins at midnight. If  $\text{timcorr} = 0$ , then  $\text{MJD} = \text{barytime} - 0.5 \text{ d}$  and  $\text{barytime} = \text{MJD} + 0.5 \text{ d}$ .

### 7.4.3 Caveats and Uncertainties

*Note 5 is new since Release 5.*

Factors which users should consider before basing scientific conclusions on time stamps are:

1. The precise phasing of an individual pixel with respect to the Cadence time stamp (not understood to better than +/- 0.5 s) at this time.
2. General and special relativistic effects in the calculation of the barycentric correction. For example, time dilation at Kepler with respect to a clock at rest with respect to the solar system barycenter, but outside the Sun's gravity well, is  $7.5 \times 10^{-9} = 0.23 \text{ s/yr}$  – so these effects cannot be dismissed out of hand at this level, and must be shown to be negligible at the level of Kepler's time accuracy requirement of 50 ms or corrected for.
3. The existing corrections have yet to be verified with flight data.
4. Light travel time and relativistic corrections to the user's target, if the target is a component of a binary system.

5. BJD as calculated in this Release is UTC based and high-precision users will want to use BJD in the Dynamical Time standard, which is the preferred absolute time reference for extra-terrestrial phenomena (See Ref. 17 for a thorough discussion).

The advice of the DAWG is not to consider as scientifically significant relative timing variations less than the read time (0.5 s) or absolute timing accuracy better than one frame time (6.5 s) until such time as the stability and accuracy of time stamps can be documented to near the theoretical limit.

## **7.5 Future Formats Under Discussion**

*This Section is unchanged since Release 4.*

The Science Office recognizes that the MAST products are deficient in several ways, and are discussing the following improvements:

1. Provision of an aperture extension, which will tell users which pixels were used to calculate uncorrected flux time series and centroids.
2. Data quality flags, encoding much of the information on lost or degraded data and systematic errors provided in these Notes in a way that will spare users the drudgery of fusing the data in the Supplement with the light curve data.
3. A local WCS coordinate system derived from linearized motion polynomials with Cadence-to-Cadence corrections from the mid-time of the data set. These corrections are a target-specific image motion time series for users to use in their own systematic error correction and are thus an improvement on the mod.out center motion time series provided in the Supplement.
4. Packaging target pixel files as columns of images rather than as pixel lists.

## 8. References

1. "Initial Assessment Of The Kepler Photometric Precision," W.J. Borucki, NASA Ames Research Center, J. Jenkins, SETI Institute, and the Kepler Science Team (May 30, 2009)
2. "Kepler's Optical Phase Curve of the Exoplanet HAT-P-7," W. J. Borucki *et al.*, *Science* Vol 325 7 August 2009 p. 709
3. "Pixel Level Calibration in the Kepler Science Operations Center Pipeline," E. V. Quintana *et al.*, SPIE Astronomical Instrumentation conference, June 2010.
4. "Photometric Analysis in the Kepler Science Operations Center Pipeline," J. D. Twicken *et al.*, SPIE Astronomical Instrumentation conference, June 2010.
5. "Presearch Data Conditioning in the Kepler Science Operations Center Pipeline," J. D. Twicken *et al.*, SPIE Astronomical Instrumentation conference, June 2010.
6. Dave Monet, private communication.
7. "Initial Characteristics of Kepler Long Cadence Data for Detecting Transiting Planets," J. M. Jenkins *et al.*, *ApJ Letters* **713**, L120-L125 (2010)
8. "Initial Characteristics of Kepler Short Cadence Data," R. L. Gilliland *et al.*, *ApJ Letters* **713**, L160-163 (2010)
9. "Overview of the Kepler Science Processing Pipeline," Jon M. Jenkins *et al.*, *ApJ Letters* **713**, L87-L91 (2010)
10. "Discovery and Rossiter-McLaughlin Effect of Exoplanet Kepler-8b," J. M. Jenkins *et al.*, submitted to *ApJ* <http://arxiv.org/abs/1001.0416>
11. "Kepler Mission Design, Realized Photometric Performance, and Early Science," D. Koch *et al.*, *ApJ Letters* **713**, L79-L86 (2010)
12. "Selection, Prioritization, and Characteristics of Kepler Target Stars," N. Batalha *et al.*, *ApJ Letters* **713**, L109-L114 (2010)
13. "Kepler Science Operations," M. Haas *et al.*, *ApJ Letters* **713**, L115-L119 (2010)
14. "The Kepler Pixel Response Function," S. Bryson *et al.*, *ApJ Letters* **713**, L97-L102 (2010)
15. "Instrument Performance in Kepler's First Months," D. Caldwell *et al.*, *ApJ Letters* **713**, L92-L96 (2010)
16. "Selecting Pixels for Kepler Downlink," S. Bryson *et al.*, SPIE Astronomical Instrumentation conference, June 2010.
17. "Achieving Better Than One-Minute Accuracy In The Heliocentric And Barycentric Julian Dates," Jason Eastman, Robert Siverd, B. Scott Gaudi, submitted to *ApJ* <http://arxiv.org/abs/1005.4415v2>

## 9. List of Acronyms and Abbreviations

ACS	Advanced Camera for Surveys
ADC	Analog to Digital Converter
ADCS	Attitude Determination and Control Subsystem
AED	Ancillary Engineering Data
ARP	Artifact Removal Pixel
BATC	Ball Aerospace & Technologies Corp.
BG	BackGround pixel of interest
BOL	Beginning Of Life
BPF	Band Pass Filter
CAL	Pixel Calibration module
CCD	Charge Coupled Device
CDPP	Combined Differential Photometric Precision
CDS	Correlated Double Sampling
CR	Cosmic Ray
CSCI	Computer Software Configuration Item
CTE	Charge Transfer Efficiency
CTI	Charge Transfer Inefficiency
DAA	Detector Array Assembly
DAP	Data Analysis Program
DAWG	Data Analysis Working Group
DCA	Detector Chip Assembly
DCE	Dust Cover Ejection
DIA	Differential Image Analysis
DMC	Data Management Center
DNL	Differential Non-Linearity of A/D converter
DSN	Deep Space Network
DV	Data Validation module
DVA	Differential Velocity Aberration
ECA	Electronic Component Assembly
EE	Encircled Energy
EOL	End of Life
ETEM	End-To-End Model of Kepler
FFI	Full Field Image
FFL	Field Flattener Lens
FGS	Fine guidance sensor
FOP	Follow-up Observation Program
FOV	Field of View
FPA	Focal Plane Assembly
FPAА	Focal Plane Array Assembly



FSW	Flight Software
GCR	Galactic Cosmic Ray
GO	Guest Observer
GUI	Graphical User Interface
HGA	high-gain antenna
HST	Hubble Space Telescope
HZ	Habitable Zone
I&T	Integration and Test
INL	Integral Non-Linearity of A/D converter
IRNU	Intra-pixel Response Nonuniformity
KACR	Kepler Activity Change Request (for additional data during Commissioning)
KAR	Kepler Anomaly Report
KCB	Kepler Control Box
KDAH	Kepler Data Analysis Handbook
KIC	Kepler Input Catalog
KSOP	Kepler Science OPERations
KTD	Kepler Tech Demo (simulated star field light source)
LC	Long Cadence
LCC	Long Cadence Collateral
LDE	Local Detector Electronics
LGA	low-gain antenna
LOS	Line of Sight
LPS	LDE Power Supply
LUT	look-up table
LV	Launch Vehicle
MAD	Median Absolute Deviation
MAST	Multi-mission Archive at STSci
MJD	Modified Julian Date = JD - 2400000.5
MOC	Mission Operation Center
MORC	Module, Output, Row, Column
NVM	Non-Volatile Memory
OFAD	Optical Field Angle Distortion
PA	Photometric Analysis module
PAD	Photometer Attitude Determination (Pipeline S/W)
PDC	Pre-Search Data Conditioning module
PID	Pipeline instance Identifier (unique number assigned to each run of the Pipeline)
PM	Primary Mirror
PMA	Primary Mirror Assembly
POI	Pixels of Interest

PPA	Photometer Performance Assessment (Pipeline S/W)
ppm	parts per million
PRF	Pixel Response Function
PRNU	Pixel Response Non-Uniformity
PSD	power spectral density
PSF	Point Spread Function
PSP	Participating Scientist Program
PWA	Printed Wiring Assembly
QE	Quantum Efficiency
RC	Reverse Clock
S/C	Spacecraft
S/W	Software
SAO	Smithsonian Astrophysical Observatory
SC	Short Cadence
SCo	Schmidt Corrector
SDA	Science Data Accumulator
SNR	Signal-to-Noise Ratio
SO	Science Office
SOC	Science Operations Center
SOL	Start-of-Line
SSR	Solid State Recorder
SSTVT	Single-String Transit Verification Test
STScI	Space Telescope Science Institute
SVD	Singular Value Decomposition
TAD	Target and Aperture Definition module
TDT	Target Definition Table
TPS	Transiting Planet Search module
TVAC	Thermal Vacuum testing

## 10. Contents of Supplement

*This Section is conceptually unchanged since Release 5 (Q0-Q1). The files themselves describe Q4 data. Changes to the MJD offset in thermal telemetry files since Release 5 are shown in red.*

The Supplement is available as a full package (DataReleaseNotes\_06\_SupplementFull.tar) and a short package suitable for emailing (DataReleaseNotes\_06\_SupplementSmall.tar). The small package does not contain the following files:

Q4M1-SC\_background.txt  
Q4M2-SC\_background.txt  
Q4M3-SC\_background.txt  
Q4-LC-MAST-R6\_background.txt  
Q4-MAST-R6\_central\_column\_motion.txt  
Q4-MAST-R6\_central\_row\_motion.txt  
Q4\_TH12LVAT\_MJD\_gap.txt  
Q4\_TH1RW34T\_MJD\_gap.txt

### 10.1 Pipeline Instance Detail Reports

These files list the Pipeline version and parameters used to process the data, so that the Pipeline results in this Release can be reconstructed precisely at some future time. Multiple files for the same data set are needed if the Pipeline needs to be re-run from a particular step, or to process anomalous modules (like mod 3 in Q4) separately. The file names are:

Q4M1\_SC\_Mod3\_pa\_pdc\_pipeline\_instance\_report\_100527.txt  
Q4M1\_SC\_excludeMod3\_pipeline\_instance\_report\_100526.txt  
Q4M2\_SC\_r6.1\_ksop479\_pre-run\_Trigger\_Report\_100609.txt  
Q4M3\_SC\_r6.1\_exclude\_mod3\_KSOP-479-Instance-Detail\_Report\_100603.txt  
Q4\_LC\_excludeMod3\_cal\_pipeline\_instance\_report\_100520.txt  
Q4\_LC\_excludeMod3\_pa\_pdc\_pipeline\_instance\_report\_100522.txt  
Q4\_SC\_Mod3\_cal\_pipeline\_instance\_report\_100525.txt

### 10.2 Thermal and Image Motion Data for Systematic Error Correction

These files are provided so that users can perform their own systematic error correction, if they conclude that the methods used by PDC are not suitable for their targets and scientific goals. It is important to remember that inclusion of additional time series to the cotrending basis set may not improve the results if the cotrending time series are noisy, poorly sampled, or nearly degenerate. The thermal AED will, in general, have to be resampled to match the Cadence times, and on physical grounds it may be more effective to cotrend against bandpass-filtered AED as separate basis vectors. See the SPIE PDC paper (Ref. 5) for a brief discussion of synchronizing ancillary data to mid-Cadence timestamps, and the use of synchronized AED as a cotrending basis set.

#### 10.2.1 Mod.out Central Motion

On rare occasions (<2% of the points), users may notice some “chatter” in the motion time series, which results from a known problem with the motion polynomial fitting algorithm and not actual jumps in telescope attitude or CCD position. A more robust, iterative algorithm has been

identified and will be implemented in future Pipeline software to remedy this problem. Users will also clearly see DVA and the signatures of the variable FGS guides stars (Section 6.2) and the reaction wheel heaters (Section 6.3.2) in the motion time series.

Files: `Q4-MAST-R6_central_column_motion.txt` and `Q4-MAST-R6_central_row_motion.txt` -- Channel central column (row) motion from motion polynomials for all channels, sampled at the Long Cadence period.

#### Column Descriptions

1. Cadence Interval Number
2. Relative Cadence Index
3. Gap Indicator. 1 = Momentum Dump or Loss of Fine Point
4. Cadence mid-Times, MJD
- 5-88. Mod.out center column (row) for each channel. Units: pixels. mod.outs are shown

`Q4-MAST-R6_central_motion.mat` -- MATLAB file containing both row and column motion; this will spare MATLAB users the drudgery of parsing the text files.

### 10.2.2 Average LDE board Temperature

`Q4_LDE_averageBoardTemp.txt` -- average of the ten LDE board temperatures.

#### Column descriptions:

1. **MJD - 55000**, units: d, sampling  $6.92E-04$  d = 59.75 s
2. Average temperature, units: C

### 10.2.3 Reaction Wheel Housing Temperature

`Q4_TH1RW34T_MJD_gap.txt` -- Reaction wheel housing temperature. Data are gapped for desats and median-filtered with a box width = 5 samples.

#### Column definitions:

1. **MJD**, units: d, sampling (unfiltered) = 58.0 s
2. TH1RW3T -- units: C
3. TH1RW4T -- units: C

### 10.2.4 Launch Vehicle Adapter Temperature

`Q4_TH1LVAT_MJD_gap.txt` -- Launch Vehicle Adapter Temperature. Data are gapped for desats and median-filtered with a box width = 5 samples.

#### Column definitions:

1. **MJD - 55000**, units: d, sampling (unfiltered) = 58.0 s
2. TH1LVAT -- units: C
3. TH2LVAT -- units: C

## 10.3 Background Time Series

The background time series provide the median calibrated background pixel value on a given mod.out and Cadence. For LC, the background pixels are the dedicated background pixel set. For SC, the background pixels are the target pixels which are not in the optimal aperture. These values are calculated directly from the pixel sets, not from the Pipeline-derived background polynomials.

Q4-LC-MAST-R6\_background.txt

Q4M1-SC\_background.txt

Q4M2-SC\_background.txt

Q4M3-SC\_background.txt

Column definitions

1. Cadence Interval Number
2. Relative Cadence Index for Argabrightening Cadences
3. Gap Indicator. 1 = No Data, Momentum Dump, or Loss of Fine Point
4. Cadence mid-Times, MJD
5. Median background current averaged over FPA, e-/Cadence. All zeros = no SC targets
- 6-89. Mod.out background in e-/Cadence for each channel. mod.outs are shown

Corresponding MATLAB files are provided to spare MATLAB users the drudgery of parsing the text files.

## **10.4 Flight System Events**

### Argabrightening Detections

ArgAgg\_Q4-R6\_LC\_PID1676\_MADT010\_MCT10\_Summary.txt

ArgAgg\_Q4M1-R6\_SC\_PID1756\_MADT010\_MCT10\_Summary.txt

ArgAgg\_Q4M2-R6\_SC\_PID2037\_MADT010\_MCT10\_Summary.txt

ArgAgg\_Q4M3-R6\_SC\_PID1876\_MADT010\_MCT10\_Summary.txt

Column Definitions:

1. Cadence Interval Number for Argabrightening Cadences
2. Relative Cadence Index for Argabrightening Cadences
3. Arg Cadence mid-Times, MJD
4. Mean SNR over Channels of Arg Event
5. Channels exceeding threshold in Arg Cadence
6. Channels exceeding default threshold in ArgCadence

### Out of Fine Point Cadence Lists

Q4M1\_SC\_isNotFinePoint.txt

Q4M2\_SC\_isNotFinePoint.txt

Q4M3\_SC\_isNotFinePoint.txt

Q4\_LC\_isNotFinePoint.txt

## **10.5 Calibration File READMEs**

The calibration file names are not listed in the headers of the light curves and target pixel files. The calibration file names listed in the FITS headers of Cadence files and FFIs are not, in

general, correct. The README files for the calibration files actually used for all releases to date are:

kplr2008072318\_gain.readme.txt

kplr2008102416\_read-noise.readme.txt

kplr2008102809\_undershoot.readme.txt

kplr2009060215\_linearity.readme.txt

kplr2009060615-mmo\_2d-black.readme.txt

kplr2009062300\_lsflat.readme.txt

kplr2009062414-MMO\_ssflat.readme.txt

They are supplied with the Release 5 Supplement and not duplicated in the Release 6 Supplement.